SPOT FIRE DISTANCE FROM BURNING TREES — A PREDICTIVE MODEL

FRANK A. ALBINI

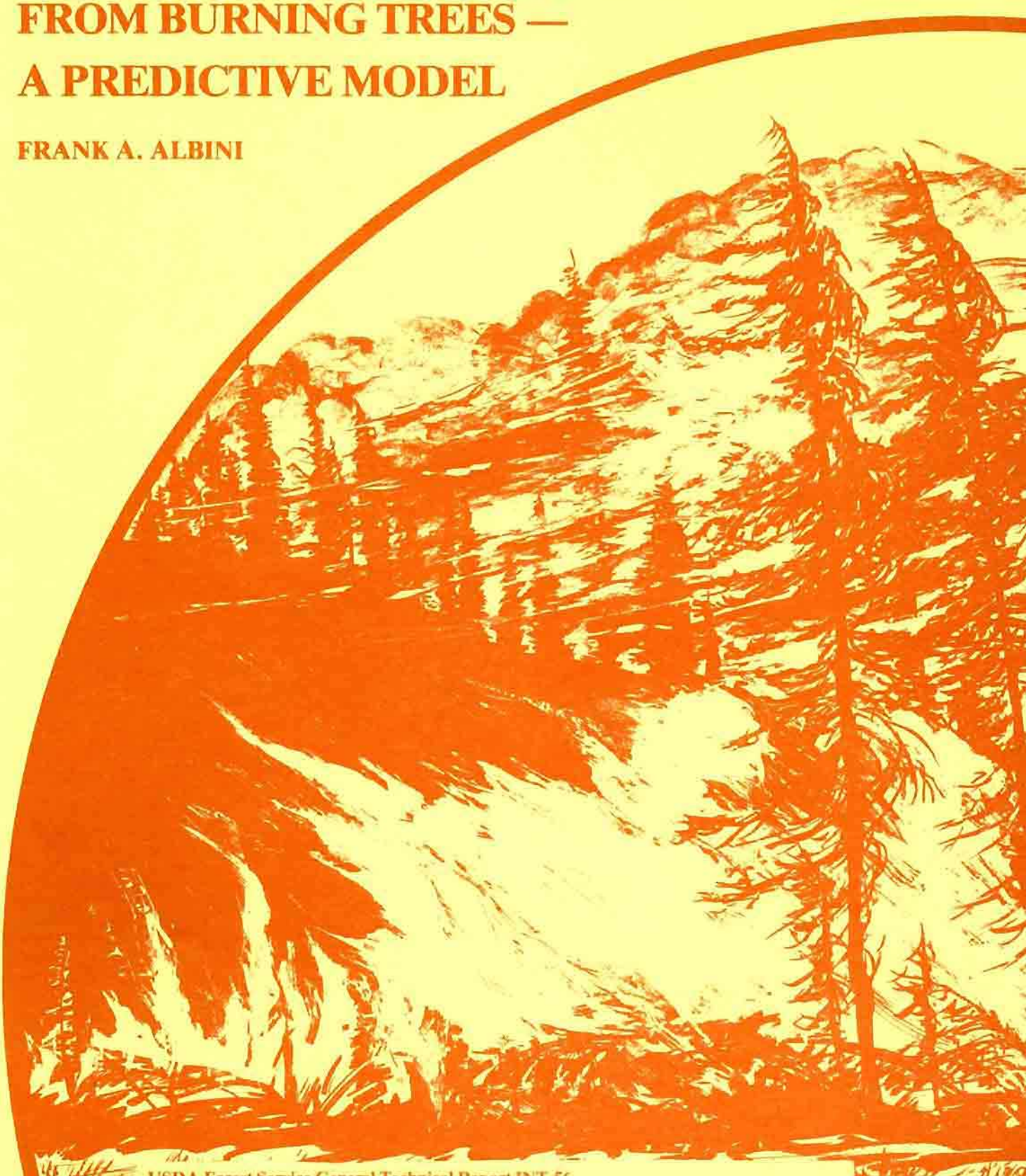

USDA Forest Service General Technical Report INT-56
INTERMOUNTAIN FOREST AND RANGE EXPERIMENT STATION
FOREST SERVICE, U.S. DEPARTMENT OF AGRICULTURE

USDA Forest Service
General Technical Report INT-56
July 1979

SPOT FIRE DISTANCE FROM BURNING TREES — A PREDICTIVE MODEL

F. A. Albini

INTERMOUNTAIN FOREST AND RANGE EXPERIMENT STATION
Forest Service
U.S. Department of Agriculture
Ogden, Utah 84401

THE AUTHOR

FRANK A. ALBINI is a Mechanical Engineer, assigned to the Fire Fundamentals research work unit at the Northern Forest Fire Laboratory in Misssoula, Montana. He earned a Ph.D. from the California Institute of Technology in 1962, where he also obtained his undergraduate training (B.S. 1958, M.S. 1959). He joined the Forest Service in October 1973 after 12 years of pure and applied research and systems analysis both in private industry and at the nonprofit Institute for Defense analyses.

ACKNOWLEDGMENTS

This model incorporates a cross section of the technical fields associated with wildland fire science. The author is indebted to specialists from several disciplines for their assistance and for educated guesswork needed to fill in pieces of the models presented here. The author accepts full responsibility for any misapplication of data or misinterpretation of theories, but wishes to acknowledge these sources:

Dr. James K. Brown - for data on foliage weights and surface/volume ratios and introduction to the literature in which such data reside.

Dr. Ralph Wilson, Jr., - for data on firebrand burning rates and consultation that helped in understanding the data.

Dr. Donald Fuquay, Mr. Robert Baughman, and Dr. Donald Latham - for encouragement, guidance, and constructive criticism in dealing with the poorly-defined meteorological aspects of this problem.

All of these people are located at the Intermountain Station's Northern Forest Fire Laboratory in Missoula, Montana.

RESEARCH SUMMARY

This paper presents a predictive model for calculating the maximum spot fire distance to be expected when firebrands are thrown into the air by the burning of tree crowns either individually or in small groups. Variables included in the model are the quantity and surface/volume ratio of foliage in the burning tree(s), the height of the tree(s), and the wind field that transports the firebrands, and the firebrand burning rate. Many aspects of the processes modeled are as yet incompletely understood and so are only weakly represented. Improved models are needed for all of the processes before predictions can be made with certainty, but a step-by-step, graphical procedure is presented here for test and evaluation in the field. No validation data are available at present.

CONTENTS

INTRODUCTION

In the jargon of forest fire control a "spot fire" is a fire set outside the perimeter of the main fire by flying sparks or embers (USDA Forest Service 1956). A wildland fire is said to be "spotting" when it produces sparks or embers that are carried by the wind and start new fires beyond the zone of direct ignition by the main fire. This type of fire spread occurs with increasing frequency as fuel moisture content declines (table 1).

Fire spread by spotting is a chance event. When it will occur and over what distance are at present unpredictable quantities that complicate the task of wildfire control. And fires ignited for desirable effects under prescribed conditions sometimes escape their intended boundaries because of spotting.

This vexing phenomenon has long challenged both the research community and fire management practitioners. This paper presents a theoretical framework and instructional materials for predicting the maximum spot fire distance from burning trees. With testing and refinement, the model given here should enable researchers and managers alike to better understand and cope with spot fires.

Problem Description

Spotting occurs over a wide range of distances, depending upon windspeed and the type (and quantity) of fuel involved in the main fire as well as fuel moisture. The severity of a potential spotting problem can be described numerically by the maximum spot fire distance to be anticipated under the conditions in question. The problem addressed in this paper arises under conditions of intermediate fire severity in which spotting distances up to a mile or two might be encountered. These burning conditions represent a rough upper limit to fire severity under which prescribed burning might be carried out. In some cases an estimate of maximum possible spotting distance may assist in delimiting prescription regimes. Large wildfires also occur frequently under burning conditions that admit intermediate-range spotting. This situation arises when fire intensity is not so high as to cause extensive crowning or crown fire spread (Van Wagner 1977), but when the intensity is sufficiently high that the fire cannot be "trusted" to burn only surface fuels (table 1).

Situations *not considered* in this work are those extreme cases in which spotting may occur up to tens of miles from the main front, as in running crown fires, fires in heavy slash or chaparral under extreme winds, and fires in which fire whirls loft burning material high into the air.

The situation treated here starts with the assumption that there occurs the occasional or sporadic "torching out" of individual trees or small groups of trees. These singular events provide the mechanism for the lofting of firebrands that are then carried by the prevailing wind. While this is not the most severe case of spread by spotting, it is a situation that often confronts planners in fire suppression and fire prescription work.

A method is sought that will permit prediction of the maximum spot fire distance to be anticipated from burning trees, given a knowledge of the terrain, forest cover, and windspeed. If maximum spotting distance can be predicted, the information might be useful in prescription writing, selecting fire control line placement, positioning of "spot chasers," and similar matters that fire managers must deal with.

Table 1.--*Spotting potential related to fuel moisture content*

(This table is based on data compiled by Hal E. Anderson, USDA Forest Service, Intermountain Forest and Range Experiment Station, Northern Forest Fire Laboratory, for Fire Behavior Officer training (National Interagency Fire Training Center, Marana Air Park, Arizona).)

Fuel moisture content			Relative ease of chance ignition, likelihood of spotting, general burning conditions
Relative humidity*	1/2-inch fuel stick	Forest litter	
- - - - - -	Percent - - - - - -		
		>25	Little or no ignition[1]
>60	>15	>20	Very little ignition;[2] some spotting may occur with winds above 9 mi/h[3]
45-60	12-15	15-19	Low ignition hazard - campfires become dangerous;[1] glowing brands cause ignition when relative humidity <50 percent[3]
40+		11-14	Medium ignitibility - matches become
30-45	7-12		dangerous;[1] "easy" burning conditions[4]
26-40		8-10	High ignition hazard - matches always dangerous;[1] occasional crowning, spotting caused by gusty winds;[2] "moderate" burning conditions[4]
15-30	5-7	5-7	Quick ignition, rapid buildup, extensive crowning; any increase in wind causes increased spotting, crowning, loss of control;[2] fire moves up bark of trees igniting aerial fuels; long distance spotting in pine stands;[3] dangerous burning conditions[4]
<15	<5	<5	All sources of ignition dangerous;[1] aggressive burning, spot fires occur often and spread rapidly, extreme fire behavior probable;[2] critical burning conditions[4]

*Relative humidity is a surrogate for "fine" fuel moisture content.

[1]Gisborne (1936)
[2]USDA Forest Serv., Northern Region (1973)
[3]Florida Div. For. (1973)
[4]Barrows (1951)

Approach to Solution

The approach used in constructing this model is to examine each phase of the process and develop a mathematical description for it. The individual "submodels" are based on physical principles to a large extent, but assumptions, approximations, and inadequately supported empirical relationships are sprinkled throughout. Each submodel provides an element of information needed to predict the maximum spot fire distance. As better theories and data become available, the submodels can be revised and improved. But the framework that links each of the submodels rests on a series of basic assumptions that form a conceptual picture of the overall process. The process modeled is the following sequence;

A tree, or a small group of trees, "torches out." The flame, and the buoyant plume above it, exist for a brief period of time. This fluid flow field is capable of lofting potential firebrands into the air. The flow structures are described by separate, steady-state models, joined at the tip of the flame. These models assume still ambient air for simplicity, and to ensure that a maximum height is predicted for the firebrand particles.

The flight of an inert wood cylinder in the flame/plume flow field serves to predict the height of a potential firebrand as a function of time. The particle is assumed to start from the top of a tree involved in the flame at the instant the flame is established. It travels vertically until the flame goes out and the flow field collapses. The height achieved by the particle depends on its diameter and density and on the flow field description.

When the particle reaches its maximum height, it is then subjected to the ambient wind field and transported laterally as it falls. The burning of the particle is accounted for by a simple empirical model that describes its falling velocity as a function of time. The maximum spot fire distance is established by requiring that the particle is totally consumed just as it returns to the ground. Smaller particles would travel farther but burn out before reaching the ground; larger ones could not travel so far.

The wind field that carries the firebrand can be modeled by a logarithmic variation with height for flat terrain (fig. 1). But another submodel is required to reflect the influence of ridges and valleys on the wind field (fig. 2).

Each of the submodels is discussed more fully in the section entitled Synopsis of Submodel Content (p. 19) and is described in appendixes A-F.

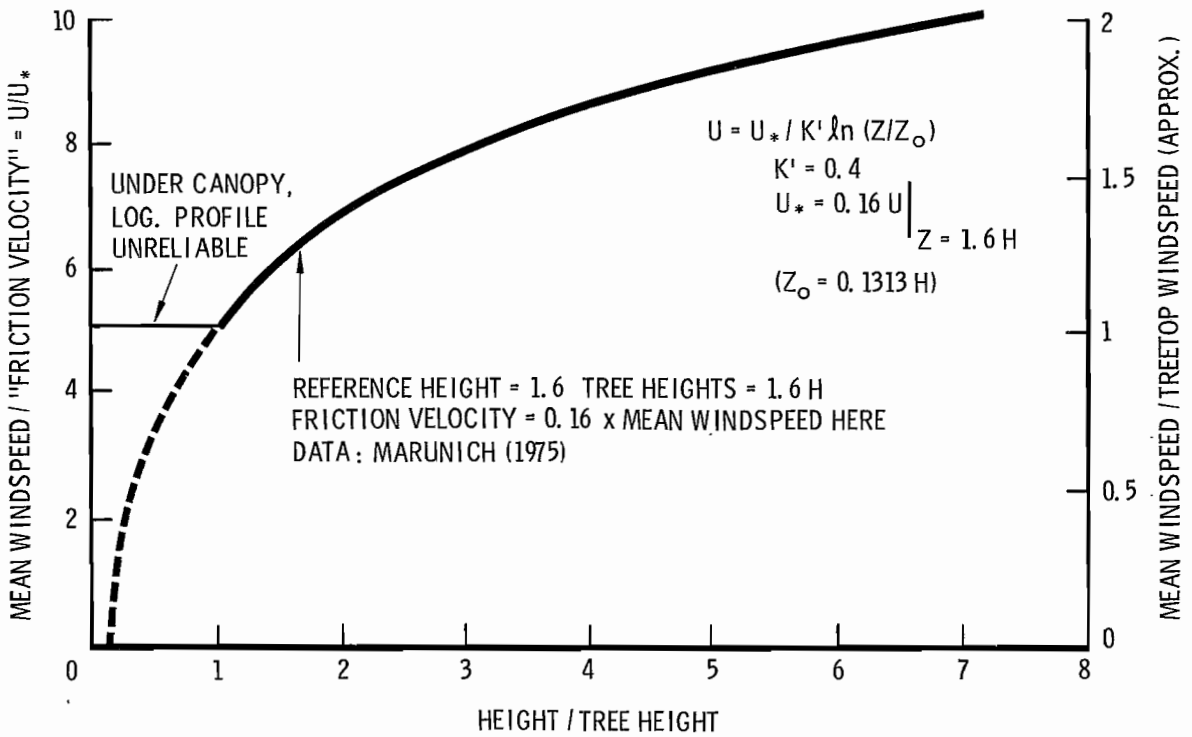

Figure 1.--Logarithmic windspeed variation with height (above uniform forest canopy).

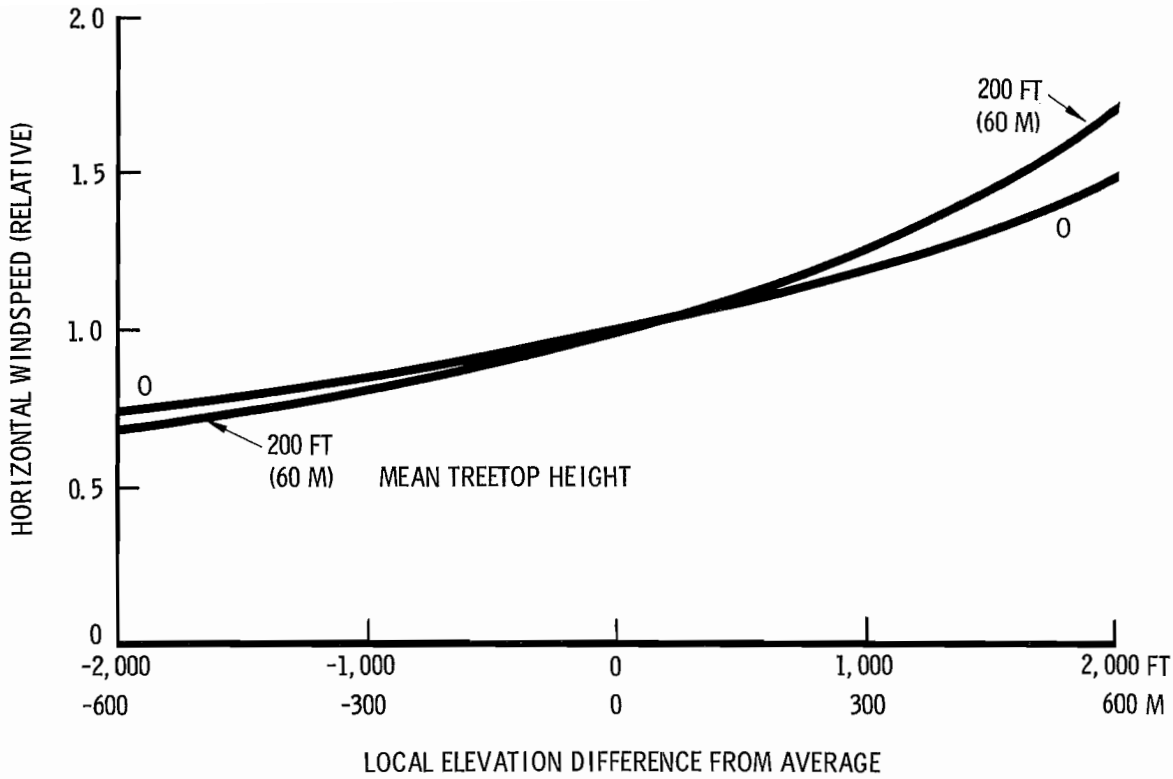

Figure 2.--Variation of horizontal windspeed (at constant height above local terrain) with elevation difference from average.

Factors Omitted in this Approach

Before this model can be applied and tested, it is essential that the user recognize what the model does not include. Several essential features of the spotting process are omitted from consideration here and no amount of adjustment of the submodels will allow them to be reflected in the results. These are factors that must be incorporated by further model development. Until this is accomplished, the user must supply the missing pieces by whatever means he can. The principal missing elements are:

1. *The likelihood of trees burning.* No consideration is included here of the probability that a tree (or group of trees) will "torch out." The type and quantity of surface fuels, the burning conditions, overstory species, crown separation, etc., all influence this factor. The model presented here must be thought of as a "what if" computation aid; the user must supply the description of the trees that are to be considered to burn as input to the model. Van Wagner (1977) describes conditions for the start and spread of crown fires. When burning conditions are so severe that crown fires are to be expected, this model would be of only marginal interest. So Van Wagner's work can be used as a guide to conditions under which one should consider the chance of torching and spotting to be significant.

2. *Availability of optimum firebrand material.* This model presumes that at least one ideally suited firebrand particle exists in an unfettered state near the top of a burning tree. This is consistent with the intention to estimate the maximum potential spot fire distance only. Any reduction in maximum spotting distance due to the fact that an ideal particle was not present is outside the scope of the model presented here. The fact that a wood cylinder is used to represent the maximum-range firebrand is not felt to be a source of significant distortion. This assumption is discussed more fully below.

3. *The probability of spot fire ignition.* In this model the maximum-range particle is idealized as just being totally consumed at the instant it reaches the ground. The fact that an extremely small spark or ember can indeed ignite forest fuels is established by experimental data,[1] so this idealization does not substantially weaken the model. But a firebrand must come into contact with easily ignited dry fuel (e.g., litter, duff, rotten wood) for a spot fire to start. This model does not deal with the chance of such contact or the probability that ignition will occur if the contact is made. Here we present only the distance that a firebrand can travel and still retain the possibility of starting a fire.

4. *The number of spot fires.* The probabilistic question of how many spot fires there might be under certain conditions, or the number per unit surface area, is not addressed here. Only when the three elements listed above are appropriately modeled will it be possible to predict the density distribution of spot fire ignitions (Muraszew and Fedele 1976).

ESTIMATING MAXIMUM SPOT FIRE DISTANCE

This section gives a step-by-step procedure for estimating maximum spot fire distance from a tree (or group of trees) that "torches out." The steps are numbered to correspond with the specimen worksheet (exhibit 1, p. 8).

1. First, record the species of tree assumed to burn, the diameter at breast height (d.b.h.) and height of the tree, and the number of trees assumed to burn simultaneously.

These data will be needed during the completion of the worksheet, and it is important that the investigator "leave some tracks" so the work can be checked or continued after interruption. Be sure to cross out the incorrect or circle the correct units of measurement when recording dimensional data. With few exceptions one is best advised to retain one system of units for each worksheet used.

[1] R. A. Wilson, Jr., and A. P. Brackebusch, personal communication of unpublished data; Northern Forest Fire Laboratory, Missoula, Mont., September 1977.

2. Consult the guide in table 2 and select from figures 3-5 the curves to use.[2] Read from the appropriate curves the steady flame height and steady flame duration for a single burning tree of the size and species of interest. Record these on the worksheet. These numbers must be revised if more than a single tree is involved in producing the flame.

3. Consult figure 6 and record the multiplying factors for flame height and duration. Note that the flame height multiplier is greater than unity and the duration factor is less than unity, so these numbers should not be confused. Carry out the indicated multiplications and record the results. It is not necessary to record more than two significant figures. For example, a duration calculated to be 3.622 should be recorded as 3.6; a flame height of 129.4 should be recorded as 130.

4. Divide the height of the burning tree (or the average height of the burning group of trees) by the adjusted flame height determined in step 3. Be sure to use the same units of measurement so the ratio will be dimensionless. Record the result and use it to select the proper curve in figure 7. The dimensionless flame duration derived in step 3 is used to enter figure 7; read the appropriate curve and record the lofted firebrand height/steady flame height value. Multiply this quantity by the adjusted steady flame height from step 3 and record the result. To this result add one-half the tree height to obtain the initial firebrand height above ground. This result is used in figure 8 (step 6).

5. The graphs for calculating spotting distance use the windspeed at treetop height at the average elevation (e.g., midslope elevation for a ridge-valley system). It is often necessary to adjust the available data on windspeed to infer this value. First, record for reference the elevation and height above terrain at the spot the windspeed value is known or estimated. Record also this reference windspeed, the average elevation, and the mean treetop height in the area downwind of the firebrand source. This mean treetop height is intended to characterize the general forest cover of the terrain as it influences the wind field that will transport a firebrand. If the area has broken forest cover, use half the treetop height of the forest-covered portion.

Subtract the average terrain elevation from the elevation where the wind was measured. Use this difference in figure 2 to estimate the ratio of windspeed at the observation point to that at the average elevation. Record this value in the blank space marked X on the worksheet.

Next, a correction may be needed for the height above the vegetation at which the reference windspeed was determined. The reference windspeed should be reduced if it was measured above the canopy top represented by the mean treetop height noted above. If so, divide the windspeed measurement height by the mean treetop height and obtain from figure 1 the windspeed ratio. Record this value in the blank space marked Y.

---

[2]Figures are given for three regions: Intermountain west, north central/northeast, and south/southeast. The literature revealed no foliage weights for west/northwest tree species. Intermountain species might serve as adequate substitutes, such as grand fir for noble, red, and Pacific silver firs, subalpine fir for white fir, western white pine for sugar pine and Monterey pine, and Ponderosa pine for Jeffrey, Coulter, and Digger pine. Species that are essentially the same, such as Ponderosa pine, Douglas-fir, or lodgepole pine, should be directly substituted until more data become available.

If the windspeed reference height is not greater than the mean treetop height, then this correction is not to be made using figure 1. Because no generally accepted procedure is known to the author for correcting windspeed measurements *upward* to treetop height, the following suggestions are offered only as interim measures and are not based upon accepted theory or specific data.[3]

Windspeed Measurement Site	*Y Value Suggested*
Open ridgetop, 20-foot anemometer tower	1.0
Open ridgetop, hand-held anemometer	.5
Forest opening, 20-foot anemometer tower	.5
Forest opening, hand-held anemometer	.4
Under canopy, hand-held anemometer	.3

Apply the corrections for elevation (X) and height above terrain (Y) by using these factors as divisors of the reference windspeed value. Enter the adjusted windspeed value on the worksheet. This is used in the next step.

6. Figure 8 is a nomograph allowing one to predict maximum spot fire distance over flat terrain with a uniform forest cover. This distance can be corrected for the effects of terrain on the wind field, so must be computed even if the terrain is not approximately flat. Two versions of figure 8 are given--8A for British units of measurement and 8B for metric units. Choose the appropriate version of the figure and proceed as follows:

a. Enter the graph on the firebrand initial height scale (from step 4), drawing a vertical line up to the curve labeled with the treetop height recorded in step 5.

b. From the intersection point (interpolated as necessary) draw a horizontal line into the left-hand panel, through to the curve labeled with the windspeed determined in step 5.

c. From the intersection point (interpolated as necessary) draw a vertical line down to the left horizontal scale. There read off the maximum spot fire distance and record on the worksheet.

The dashed lines on the figure illustrate these steps.

7. If the terrain over which the firebrand would fly has a substantial variation in elevation, the flat-terrain spot distance can be corrected by the use of the graphs in figure 9. First, determine which description best fits the location of the firebrand source: midslope on the leeward side of a ridge (figure 9A), the valley floor (figure 9B), midslope on the windward side of a ridge (figure 9C), or ridgetop (figure 9D). Next, record the elevation difference from ridgetop to valley bottom and the distance from ridgeline to valley bottom as would be shown on a map. Divide the flat terrain spot distance from step 6 by the ridge-to-valley distance and record the result. Use this quantity in the appropriate version of figure 9 to determine the ratio of spotting distance in sinusoidal terrain to that over flat terrain. Multiply this number by the flat-terrain spotting distance from step 6 and record the result. This result is the maximum spot fire distance as would be shown on a map.

---

[3]Albini, F. A. and R. G. Baughman. Estimating windspeeds for predicting wildland fire behavior. USDA For. Serv. Res. Paper INT-211, 12 p. Intermt. For. and Range Exp. Stn., Ogden, Utah.

WORKSHEET FOR ESTIMATING MAXIMUM SPOT FIRE DISTANCE

1. Describe tree(s) assumed to torch out.

   Species_____ DBH_____(cm-in) Height_____(m-ft) Number simultaneous_____
   ↑ (use in step 2) ↑ (use in step 4)↑ (use in step 3, fig 6)↑
   See table II for number of figure to use in step 2.

2. The steady flame from one burning tree.

   From fig (3A-4A-5A): Flame height_____(m-ft). From fig (3B-4B-5B): Duration_____

3. From fig 6: Flame height multiplier_____. From fig 6: Flame duration multiplier_____

   Adjusted values: steady flame height_____(m-ft). Steady flame duration_____
   (use in step 4) ↑ (use in step 4, fig 7)↑

4. Tree height (step 1) ÷ Adjusted steady flame height (step 3) = _____(use in fig 7)

   From fig 7: Lofted firebrand height/steady flame height_____.

   Multiply by adjusted steady flame height (step 3). Result: _____(m-ft)

   Add 1/2 tree height (recorded in step 1). Result: _____(m-ft)(use in step 6, fig 8)

5. Windspeed adjustments. Record for reference:

   At elevation _____(m-ft) at height_____(m-ft) windspeed is_____(km/h-mi/h)

   Avg. elevation_____(m-ft). Mean treetop height along firebrand path_____(m-ft)

   Difference = _____(m-ft) (use in fig 2) (use in fig 2 and step 6, fig 8)↑

   From fig 2: windspeed relative to value at same height but at avg. elevation_____(X)

   Windspeed reference height ÷ mean treetop height = _____(use in fig 1 if greater than 1)

   See instructions for step 5 (use of fig 1 may not be indicated)

   From fig 1, or by estimate, windspeed at reference height relative to treetop_____(Y)

   Divide reference windspeed by (X) and result by (Y). Result_____(km/h-mi/h)
   (use in fig 8)↑

6. From fig 8(A-B): Maximum spot distance over flat terrain_____(km-mi)

7. Correct for terrain relief along flight path if necessary.
   Firebrand source is located nearest to:

   Leeward midslope_____ valley floor_____ windward midslope_____ ridgetop_____
   Use fig no: 9A 9B 9C 9D

   Elevation difference from ridge to valley_____(m-ft)

   Distance from ridge to valley as would be shown on map_____(km-mi)

   Spot distance from step 6 ÷ ridge-to-valley distance = _____(use in fig 9)

   From fig 9(A-B-C-D): Spot distance in sinusoidal terrain/flat terrain distance_____

   Multiply by maximum spot distance over flat terrain (step 6).

   Result:_____km-mi)
   This is the maximum spot distance (as shown on map) estimate ↑

EXHIBIT 1. SPECIMEN WORKSHEET

Table 2.--*Data source list and key to figures for obtaining steady flame height and duration for a single burning tree*

Region	Tree species	Data source (Foliage weight)	Figures	Curve
INTERMOUNTAIN WEST		Brown 1977	3A, 3B	
	Douglas-fir			DF
	Engelmann spruce			ES
	Grand fir			GF
	Lodgepole pine			LP
	Ponderosa pine			PP
	Subalpine fir			AF
	Western hemlock			WH
	Western red cedar			WRC
	Western white pine			WP
NORTH CENTRAL/NORTHEAST			4A, 4B	
	Balsam fir	Baskerville 1965A		BF
	Black spruce	Weetman and Harland 1964		BS
	Jack pine	Brown 1965		JP
	Red pine (North Cent.)	Brown 1965		RPC
	Red pine (Northeast)	Kittredge 1944		RPE
	Scots Pine	Ovington and Madgwick 1959		SP
	White spruce	Baskerville 1965B		WS
SOUTH/SOUTHEAST			5A, 5B	
	Loblolly pine	Rogerson 1964		LBP
	Longleaf pine	Taras and Clark 1977[1]		LLP
	Pond pine	Wendell 1960		PP
	Shortleaf pine	Loomis and others 1966		SLP
	Slash pine	Johansen and McNab 1977		SP

[1]The relationship reported by Taras and Clark requires tree height as well as diameter at breast height. Tree height was approximated by a regression of data on shortleaf pine reported by Clark and Taras (1976).

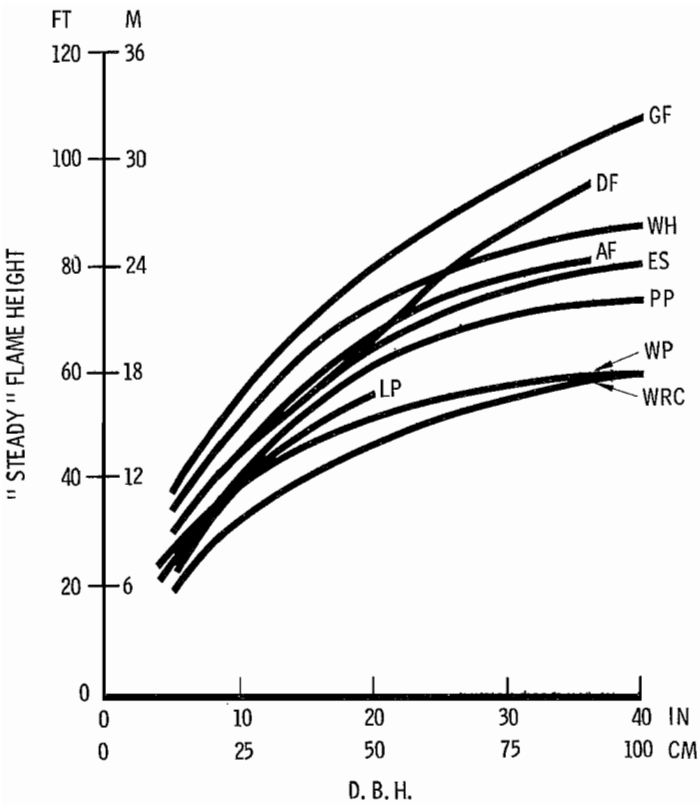

Figure 3a.--Height of "steady" flame from burning of one tree corwn in still air, for several species of trees common to the intermountain area, Western U.S.A.

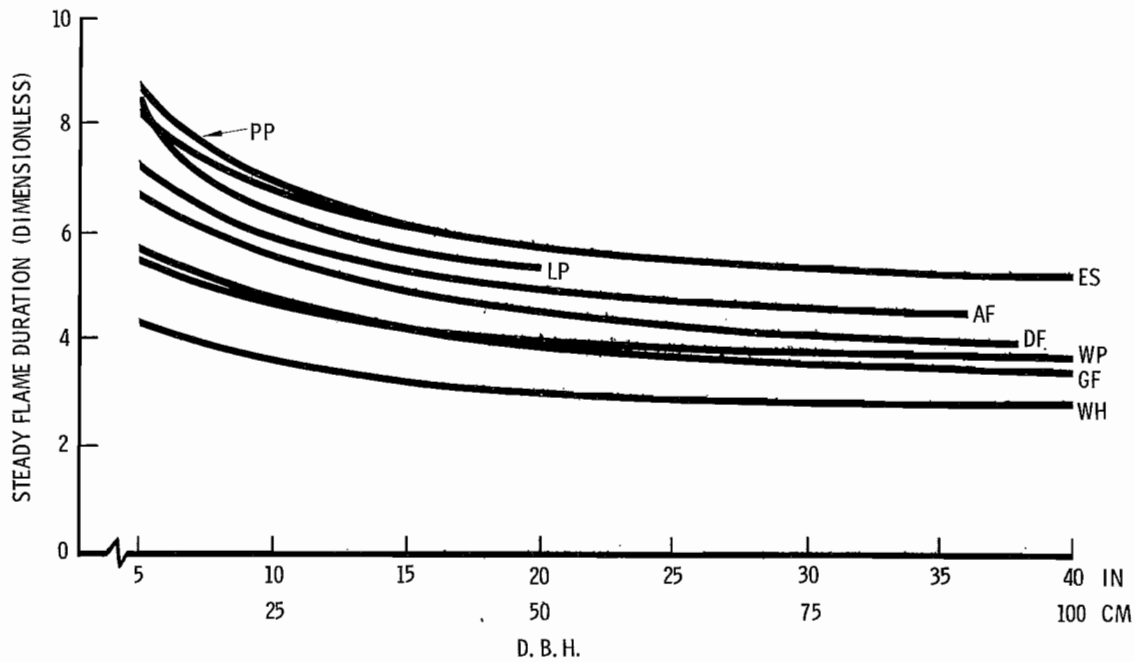

Figure 3b.--Steady flame duration for individual tree "torching out."

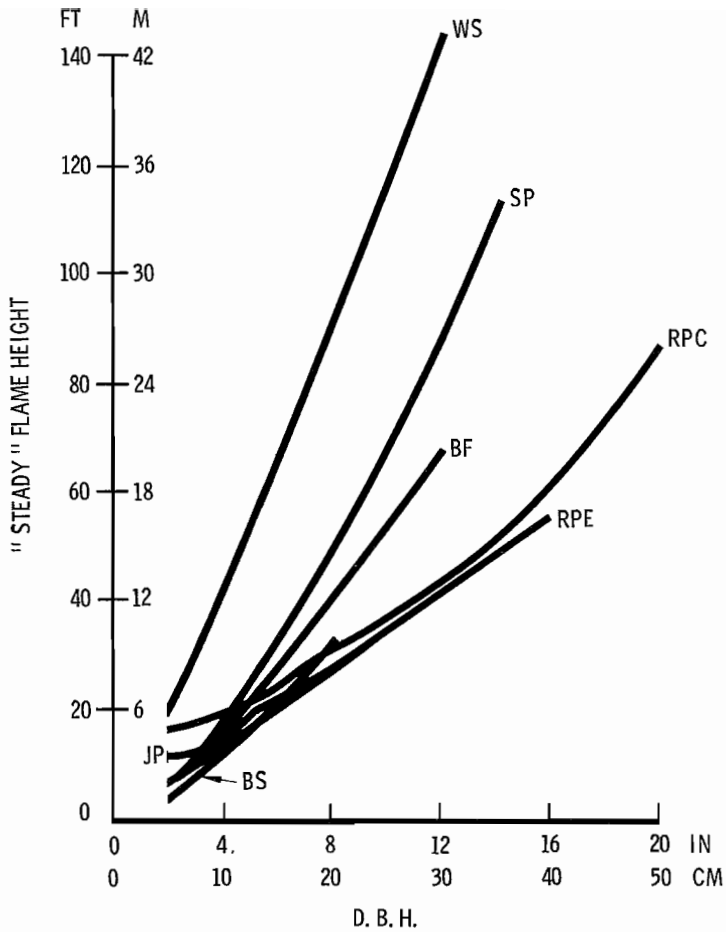

Figure 4a.--Height of "steady" flame from burning of one tree crown in still air for several species common to the North Central/Northeast U.S.A.

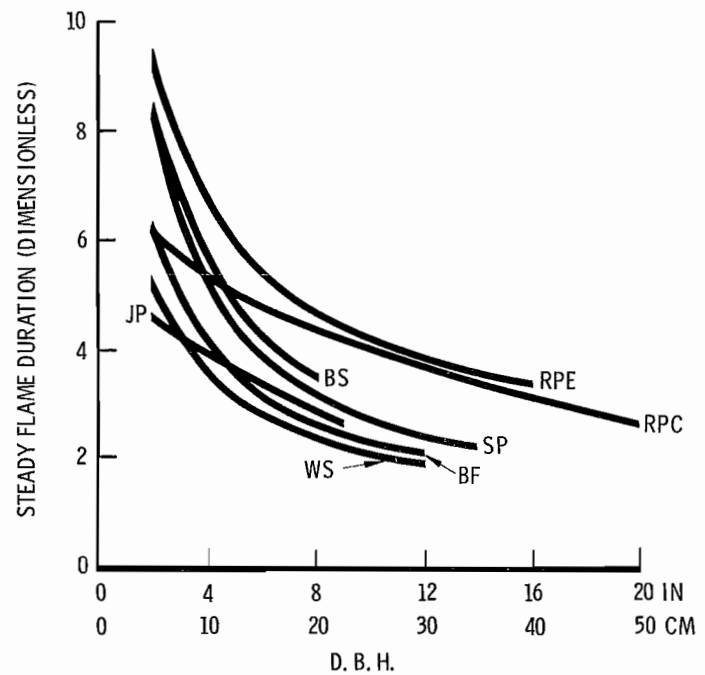

Figure 4b.--Steady flame duration for individual tree "torching out."

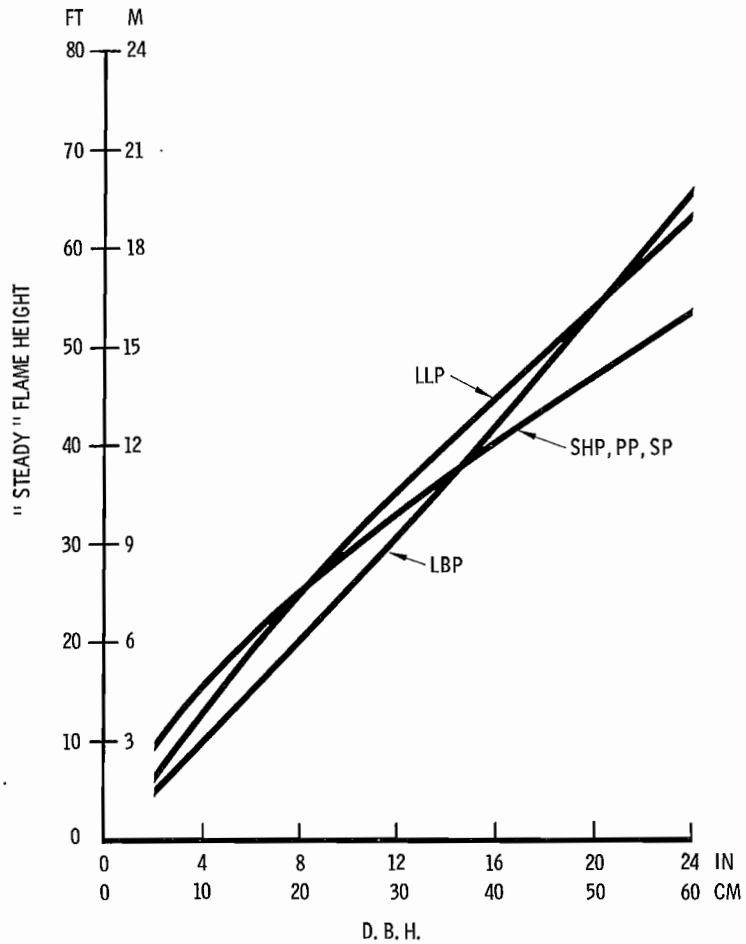

Figure 5a.--Height of "steady" flame from burning of one tree crown in still air for several Southern/Southeastern pine species.

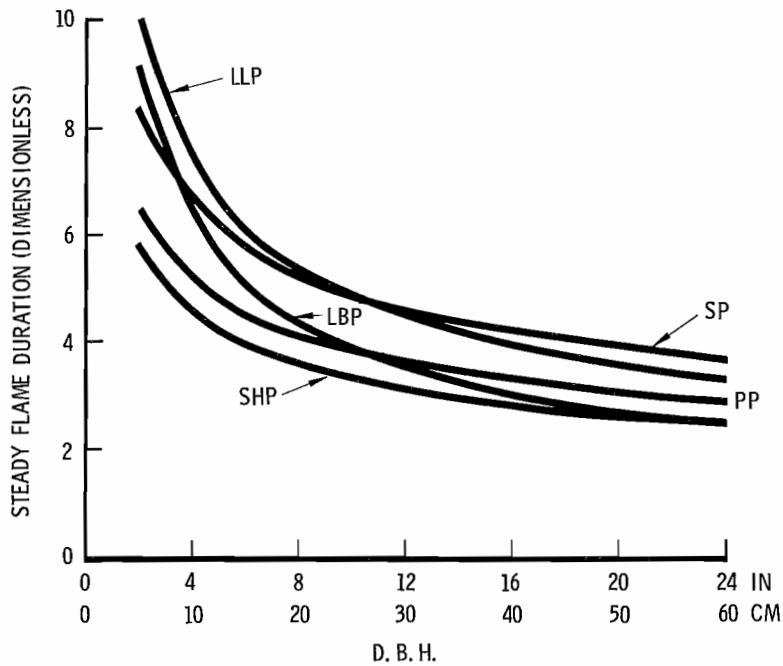

Figure 5b.--Steady flame duration for individual tree "torching out."

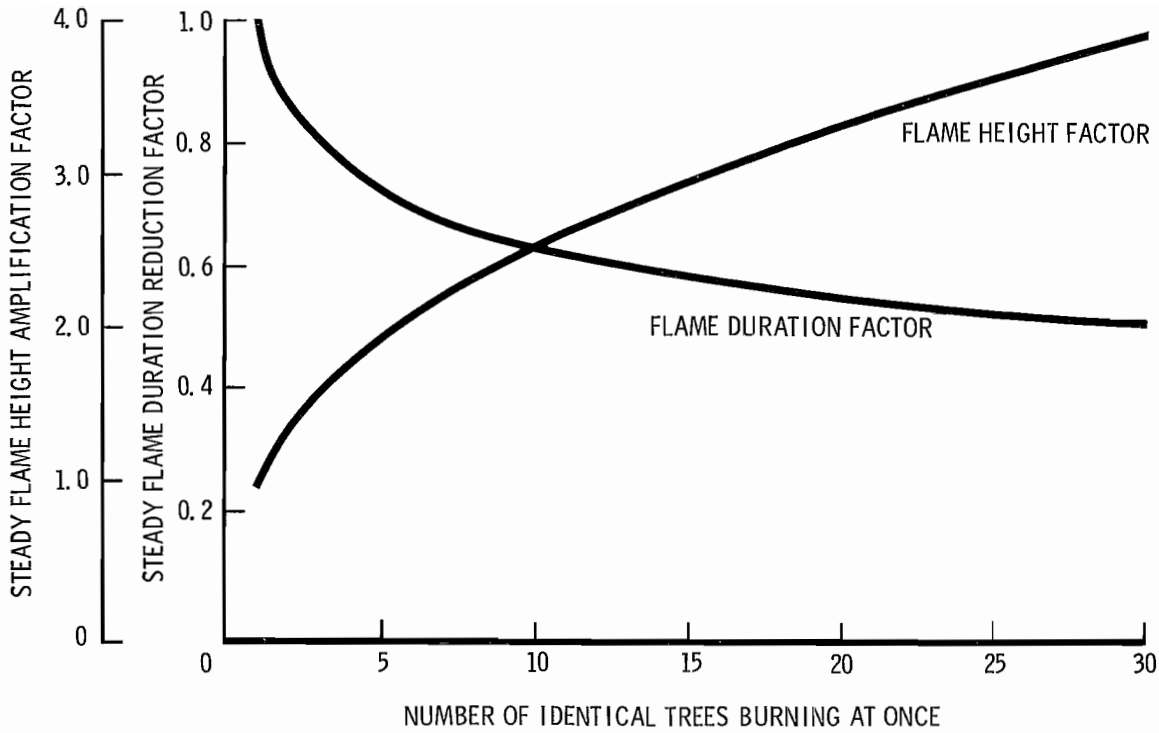

Figure 6.--Multiplication factors for flame height and dimensionless duration to account for simultaneous burning of several identical trees that produce a single steady flame and buoyant plume structure.

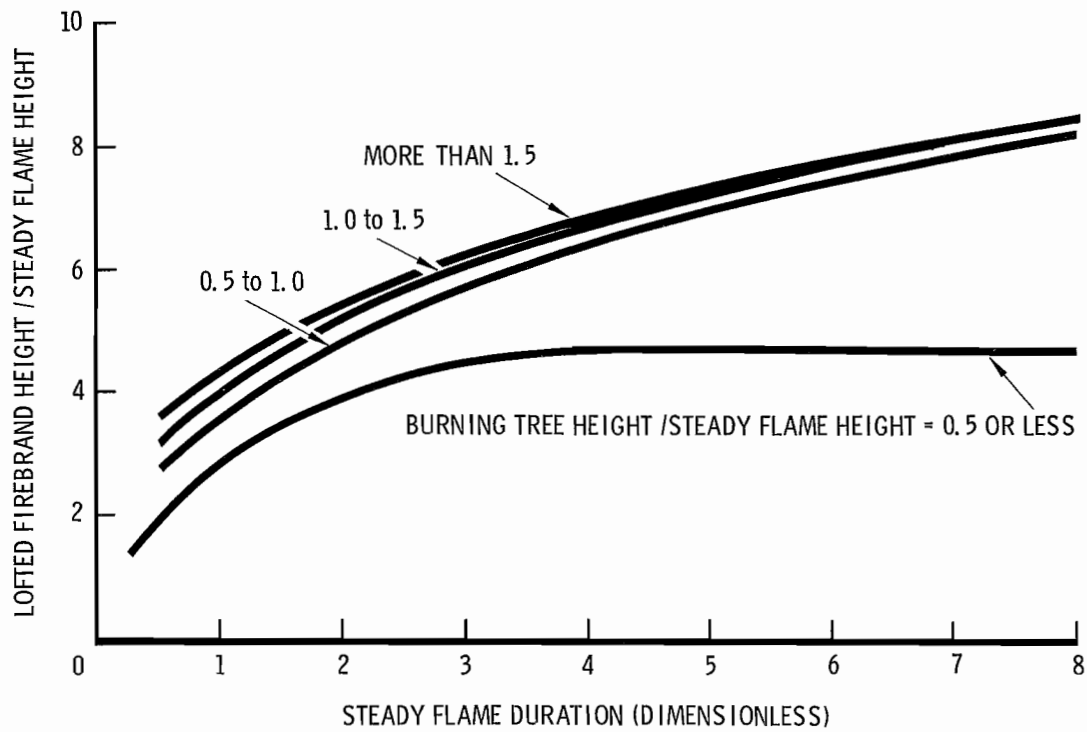

Figure 7.--Height of firebrands lofted by burning trees.

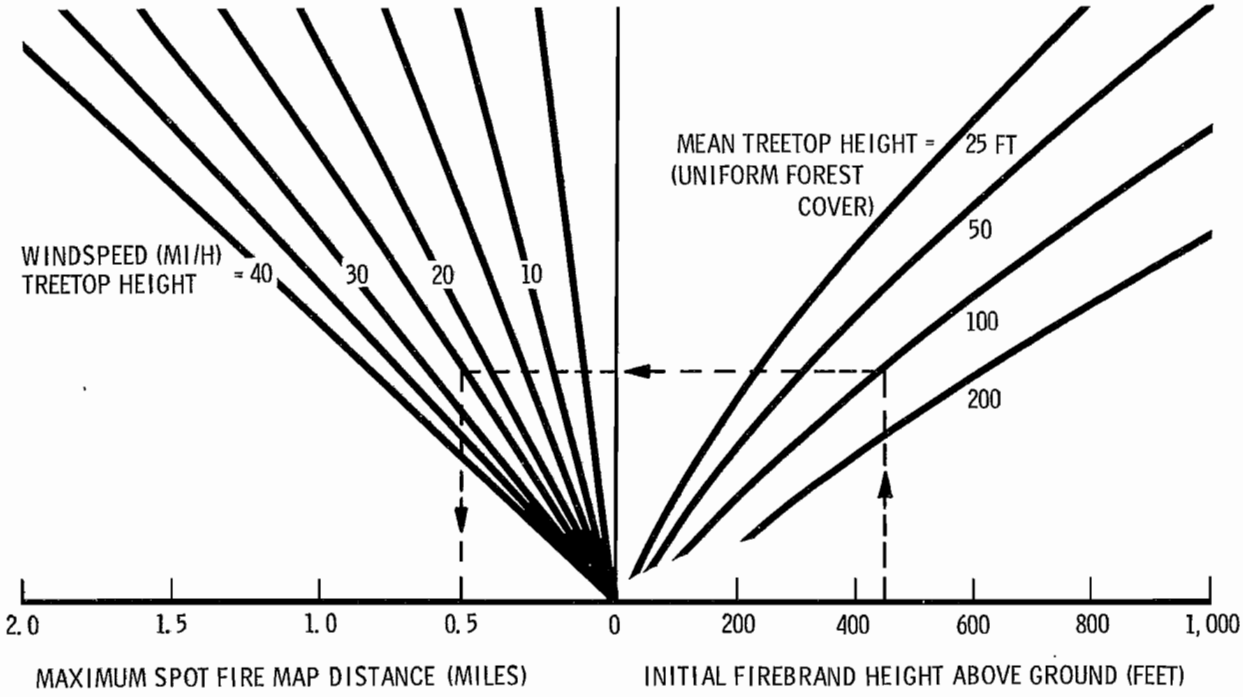

Figure 8a.--Nomograph for predicting maximum spot fire distance over flat terrain; British units of measure.

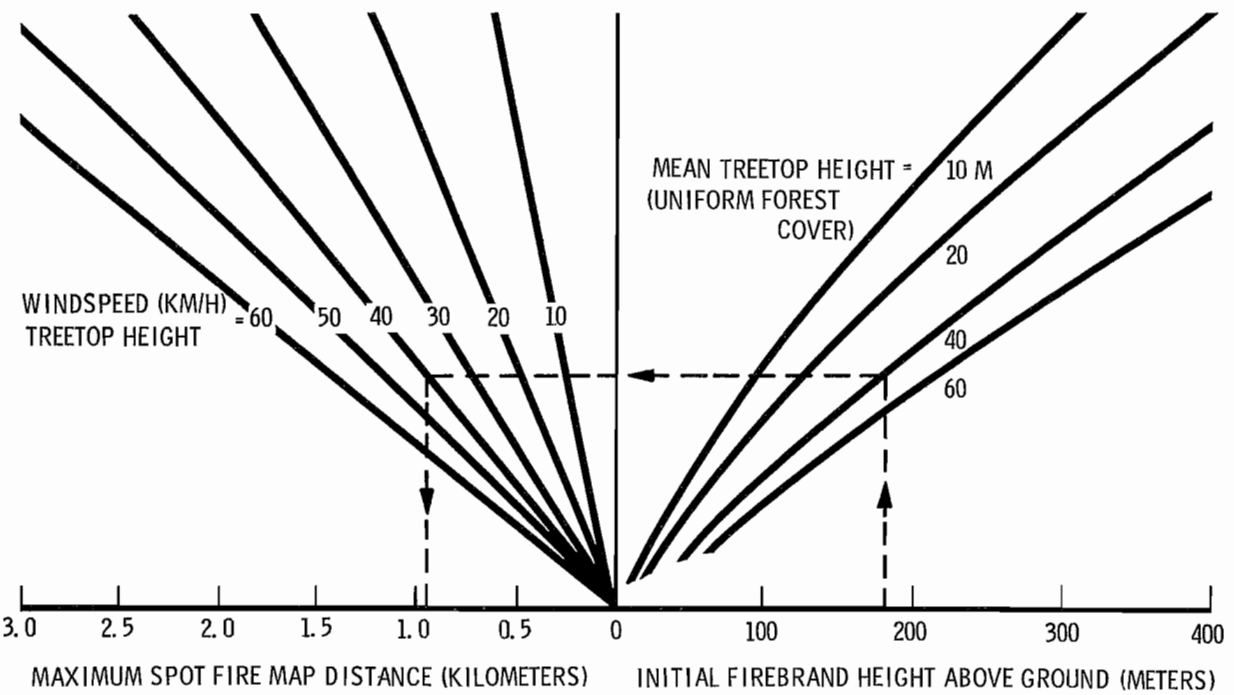

Figure 8b.--Nomograph for predicting maximum spot fire distance over flat terrain; metric units of measure.

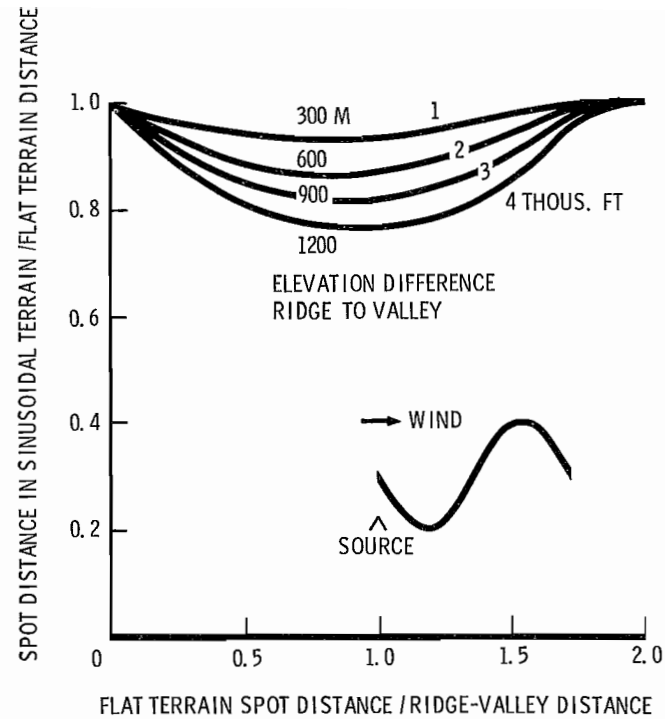

Figure 9a.--Spotting distance multiplier for sinusoidal terrain relative to flat terrain. Spot source is at midslope on leeward side. Reference wind profile is the same as the midslope profile.

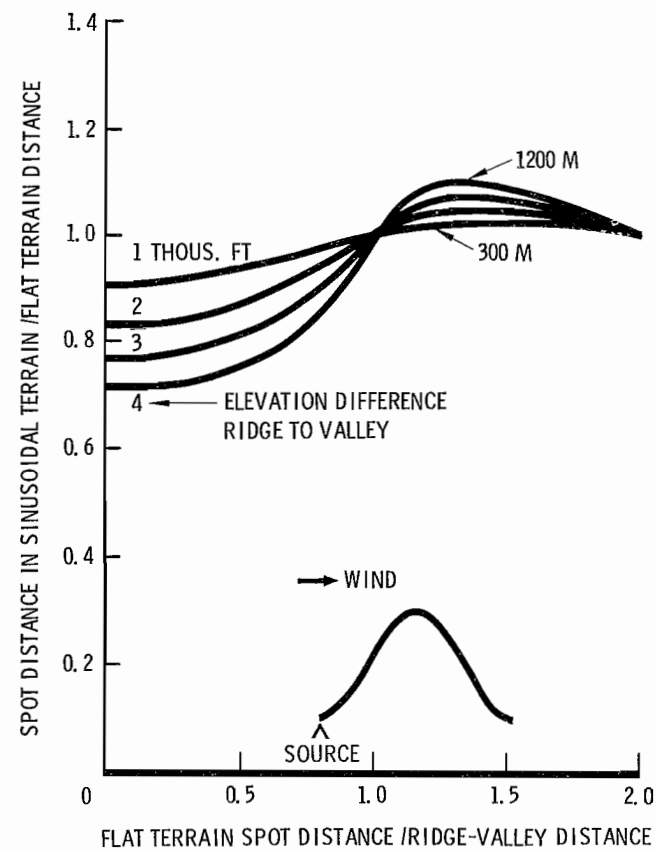

Figure 9b.--Spotting distance multiplier for sinusoidal terrain relative to flat terrain. Spot source is at valley bottom. Reference wind profile is the same as the midslope profile.

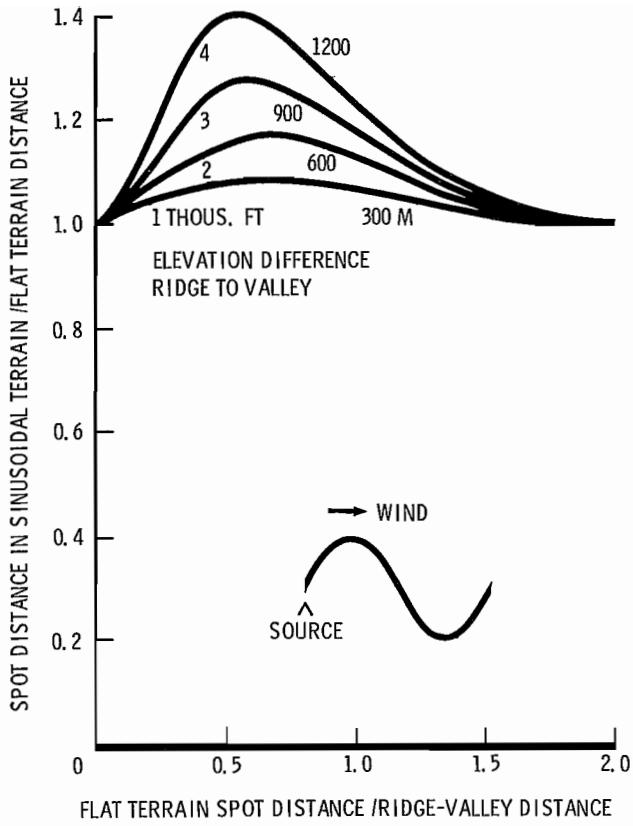

Figure 9c.--Spotting distance multiplier for sinusoidal terrain relative to flat terrain. Spot source is at midslope on windward side. Reference wind profile is the same as the midslope profile.

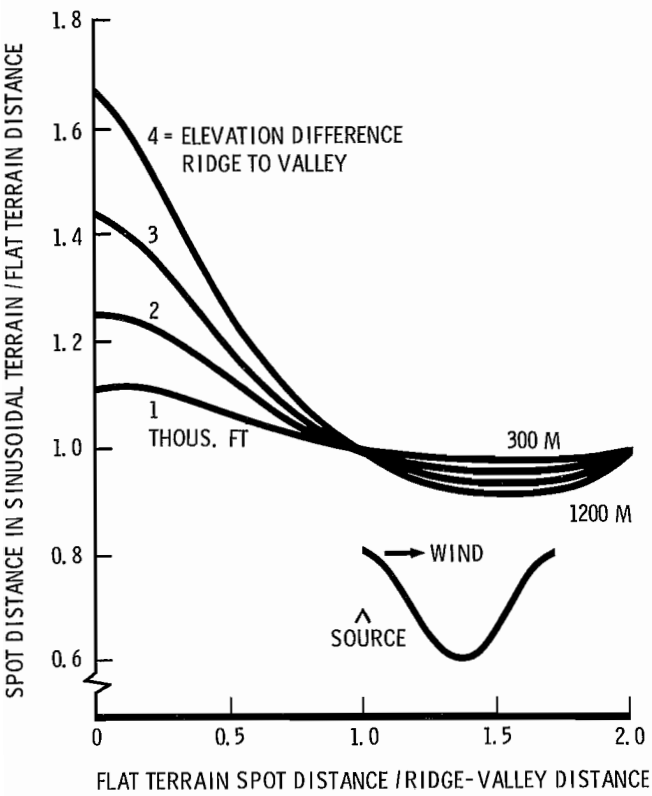

Figure 9d.--Spotting distance multiplier for sinusoidal terrain relative to flat terrain. Spot source is at ridgetop. Reference wind profile is the same as the midslope profile.

EXAMPLES

Two examples are given to help familiarize the reader with computation procedures. From the statements of the problems one can obtain all the information necessary to complete the worksheets as shown. The reader is encouraged to reconstruct the process to see how each number is used.

Example 1. A recurrent fire control problem on the Coconino National Forest near Flagstaff, Arizona, is spotting when thickets of small Ponderosa pine torch out under strong wind. Estimate maximum spot fire distance if a group of 20 trees, each 6 inches in diameter, torches out when the windspeed is 20 mi/h, measured at the nearest Fire-Danger Rating station (i.e., a 20-foot tower anemometer in a clearing). The trees that torch out are about 50 feet tall; the terrain can be considered flat with broken cover of 50-foot trees.

This problem is shown in the completed worksheet of exhibit 2. Note that in step 5 no windspeed correction for height above terrain was necessary, since the 20-foot tower windspeed is close to the "mean treetop height" (25 feet).

WORKSHEET FOR ESTIMATING MAXIMUM SPOT FIRE DISTANCE

1. Describe trees(s) assumed to torch out.
   Species Ponderosa Pine (use in step 2) † DBH 6 (cm-(in)) Height 50 (m-(ft)) (use in step 4)† Number simultaneous 20 (use in step 3, fig 6)†
   See table II for number of figure to use in step 2.

2. The steady flame from one burning tree.
   From fig ((3A)-4A-5A): Flame height 29 (m-(ft)) From fig (3B)-4B-5B): Duration 8.2
   From fig 6: Flame height multiplier 3.25. From fig 6: Flame duration multiplier .55

3. Adjusted values: Steady flame height 94 (m-(ft)). (use in step 4) † Steady flame duration 4.5 (use in step 4, fig 7)†

4. Tree height (step 1) ÷ Adjusted steady flame height (step 3) = .53 (use in fig 7)
   From fig 7: Lofted firebrand height/steady flame height 6.6.
   Multiply by adjusted steady flame height (step 3). Result: 620 (m-(ft))
   Add 1/2 tree height (recorded in step 1). Result: 650 (m-(ft)) (use in step 6, fig 8)

5. Windspeed adjustments. Record for reference:
   At elevation — (m-ft) at height 20 (m-(ft)) windspeed is 20 (km/h-(mi/h))
   Avg. elevation — (m-ft). Mean treetop height along firebrand path 25 (m-(ft)) (use in fig 2 and step 6, fig 8)†
   Difference = — (m-ft) (use in fig 2)
   From fig 2: windspeed relative to value at same height but at avg. elevation 1 (X)
   Windspeed reference height ÷ mean treetop height = 0.8 (use in fig 1 if greater than 1)
   See instructions for step 5 (use of fig 1 may not be indicated)
   From fig 1, or by estimate, windspeed at reference height relative to treetop 1 (Y)
   Divide reference windspeed by (X) and result by (Y). Result 20 (km/h-(mi/h)) (use in fig 8)†

6. From fig 8(A-B): Maximum spot distance over flat terrain .92 (km-(mi))

7. Correct for terrain relief along flight path if necessary. FLAT
   Firebrand source is located nearest to:
   Leeward midslope ____ valley floor ____ windward midslope ____ ridgetop ____
   Use fig no: 9A 9B 9C 9D
   Elevation difference from ridge to valley ____ (m-ft)
   Distance from ridge to valley as would be shown on map ____ (km-mi)
   Spot distance from step 6 ÷ ridge-to-valley distance = ____ (use in fig 9)
   From fig 9(A-B-C-D): Spot distance in sinusoidal terrain/flat terrain distance ____
   Multiply by maximum spot distance over flat terrain (step 6).
   Result: .92 (km-(mi))
   This is the maximum spot distance (as shown on map) estimate†

EXHIBIT 2. EXAMPLE 1 COMPLETED

Example 2. While a wildfire is topping out on a ridge 3,000 feet above a river valley, fire scouts note that groups of 5 to 10 large Douglas-firs are torching out sporadically. These trees are near the ridgetop and flying embers may be borne across the river, about one-half mile from the ridge. The trees are probably 100 feet tall, and appear to be in the 24-30 inch d.b.h. range. The fire weather forecaster estimates the windspeed over the ridgetop to be 15-20 mi/h (presumably at treetop height). The hillside is uniformly forested with trees averaging 75 feet in height. As fire behavior officer, you are asked if you think a crew or two should be dispatched to the far side of the river to extinguish spot fires. Assuming that the humidity is low so potential spot fires can be easily ignited, what would your answer be?

This example is shown in exhibit 3. Note that the "high end" numbers are used in each case to get a maximum estimate of spot distance. So the trees are assumed to be 30 inches d.b.h., and groups of 10 are assumed to burn at one time.

WORKSHEET FOR ESTIMATING MAXIMUM SPOT FIRE DISTANCE

1. Describe tree(s) assumed to torch out.
   Species Douglas-Fir DBH 30 (cm-(in)) Height 100 (m-(ft)) Number simultaneous 10
   (use in step 2) (use in step 4) (use in step 3, fig 6)
   See table II for number of figure to use in step 2.

2. The steady flame from one burning tree.
   From fig (3A)-4A-5A): Flame height 87 (m-(ft)) From fig (3B)-4B-5B): Duration 4.0

3. From fig 6: Flame height multiplier 2.5. From fig 6: Flame duration multiplier .63
   Adjusted values: steady flame height 220 (m-(ft)). Steady flame duration 2.5
   (use in step 4) (use in step 4, fig 7)

4. Tree height (step 1) ÷ Adjusted steady flame height (step 3) = .45 (use in fig 7)
   From fig 7: Lofted firebrand height/steady flame height 4.2.
   Multiply by adjusted steady flame height (step 3). Result: 920 (m-(ft))
   Add 1/2 tree height (recorded in step 1). Result: 970 (m-(ft)) (use in step 6, fig 8)

5. Windspeed adjustments. Record for reference:
   At elevation 3000 (m-(ft)) at height 75 (m-(ft)) windspeed is 20 (km/h-(mi/h))
   Avg. elevation 1500 (m-(ft)). Mean treetop height along firebrand path 75 (m-(ft))
   (use in fig 2 and step 6, fig 8)
   Difference = 1500 (m-(ft)) (use in fig 2)
   From fig 2: windspeed relative to value at same height but at avg. elevation 1.4 (X)
   Windspeed reference height ÷ mean treetop height = 1.0 (use in fig 1 if greater than 1)
   See instructions for step 5 (use of fig 1 may not be indicated)
   From fig 1, or by estimate, windspeed at reference height relative to treetop 1 (Y)
   Divide reference windspeed by (X) and result by (Y). Result 14 (km/h-(mi/h))
   (use in fig 8)

6. From fig 8(A-B): Maximum spot distance over flat terrain 0.64 (km-(mi))

7. Correct for terrain relief along flight path if necessary.
   Firebrand source is located nearest to:
   Leeward midslope ____ valley floor ____ windward midslope ____ ridgetop X
   Use fig no: 9A 9B 9C (9D)
   Elevation difference from ridge to valley 3000 (m-(ft))
   Distance from ridge to valley as would be shown on map 0.5 (km-(mi))
   Spot distance from step 6 ÷ ridge-to-valley distance = 1.3 (use in fig 9)
   From fig 9(A-B-C-(D)): Spot distance in sinusoidal terrain/flat terrain distance .95
   Multiply by maximum spot distance over flat terrain (step 6).
   Result: 0.61 (km-(mi))
   This is the maximum spot distance (as shown on map) estimate

EXHIBIT 3. EXAMPLE 2 COMPLETED

SYNOPSIS OF SUBMODEL CONTENT

The individual submodels of the prediction scheme are described in detail in the series of appendixes following. This section describes how the submodel results are fitted together and discusses some key assumptions used in developing the prediction scheme.

The steady flame structure submodel (appendix A) is a crude phenomenological description, predicting flame height to be proportional to the rate of fuel consumption raised to the power 2/5. Using this model to describe the flame from a burning tree requires that further assumptions be made. The assumptions used here are:

1. The fuel consumption rate is approximated as 70 percent of the dry weight of the crown foliage divided by a burning time fixed by the surface/volume ratio of the foliage. The factor 0.7 is an arbitrary estimate of the amount of foliage burned during the "steady" flaming period when the entire tree crown is involved in fire. The burning time formula is based on an empirical rule determined by Anderson (1969). Crown foliage weight can be predicted for many tree species from diameter at breast height (Keays 1971; Brown and others 1977).

2. The height of the base of the flame is not well defined. The steady flame model pictures the flow of combustible fuel gas through a horizontal orifice. The height of such an equivalent fuel supply plane is clearly between the ground and the top of the tree. This height represents the vertical displacement of the origin of the coordinate system in which the flame structure is described. In this presentation the origin is taken to be at half the tree height.

3. When several trees are consumed nearly simultaneously to produce a single large flame structure, the firebrand-lifting capability is increased. The flame height increase factor is taken to be $N^{2/5}$, implying merely a pooling of the combustible gases from N burning trees. Flames from neighboring fires will merge into a single structure when the flame heights are significantly greater than the distance separating them (Thomas and others 1965). By assuming that the flames always merge, we clearly follow the intention of analyzing the "worst case." The merging of the flames results in a reduction of the *dimensionless* flame duration, because the normalizing time is the time required for gas to pass through the flame structure. As the flame height, z_F, increases, this travel time increases as $z_F^{1/2}$. But the actual burning period stays constant, so the dimensionless measure of flame duration decreases as $N^{-1/5}$.

The buoyant plume above the steady flame is modeled (appendix B) as a self-similar, radially symmetrical, turbulent buoyant jet. The velocity and buoyancy flux are matched at the flame tip. The rest of the flow description is obtained immediately by application of well-established scaling laws. So closely related are the flame structure and plume structure models that the flame height serves to scale the plume geometry. The characteristic gas transit time also serves naturally to nondimensionalize the time history of the collapse of the plume when the fire burns out. So if the flame structure model is revised, the plume flow model will be automatically adjusted if the flame tip gas velocity scales as $z_F^{1/2}$.

The firebrand burning rate model (appendix C) used in this theory is quite similar in form to one inferred by others (Lee and Hellman 1970, Tarifa and others 1965, 1967). Numerical comparisons are difficult, however, and there is a great deal of scatter in the supporting data. This model predicts that a freely falling, burning cylinder or plate will fall at a velocity (relative to the vertical component of windspeed) that declines linearly in time. This prediction, coupled with the results from a wind field model (appendix E) that streamlines parallel the terrain, leads to a great simplification in determining the maximum possible spot fire distance.

While firebrand materials other than cylindrical stem sections are obvious candidates for analysis (Clements 1977), only minor differences in spot distance would result unless the burning rate behavior departs substantially from that used in this model. The height to which a particle will be lofted by the flame/plume flow (appendix D) depends upon the parameter group $\rho D/C_D$, where ρ is the particle mean mass density, D is a linear dimension of the particle parallel to its velocity relative to the gas flow, and C_D is the particle's drag coefficient. The time history of this same parameter group determines how far it will be borne by a given wind field.

Stemwood segments, needles, bark flakes, and seed-cone scales will behave quite similarly in this regard and a cylinder makes a good generic representative. Twigs with foliage attached, open whole seed cones, and clumps of moss are examples of potential firebrands that might behave differently. But even open seed cones would have substantially higher initial falling velocities than small-diameter stemwood segments (Clements 1977) so would not be carried nearly so high in the flow and could not travel as far. Moss clumps, on the other hand, could be lofted high into the air because the mean density of a highly porous clump is very low. But the "staying power" of a burning moss clump would be determined by the surface/volume ratio of the material and it usually would be consumed before returning to the ground.

A twig with foliage attached might be able to outdistance a simple wood cylinder, however. During the lofting phase of its flight it could have a low value of $\rho D/C_D$ because of a porous overall structure. But the foliage might soon be burned away, leaving a wood cylinder with a substantially higher value of ρD than the composite structure had. This would allow the particle sufficient lifetime to return to the ground before being consumed and it would start falling from a height that it could not achieve without the added drag area afforded by the foliage. Such a "two stage" firebrand presents a difficult analytical challenge--one that has not been met fully here. A cursory attempt to establish a range increase failed.

Samples of live twigs with needles attached were gathered and analyzed by the author. Four species of tree were represented in the samples: lodgepole pine, ponderosa pine, Douglas-fir, and Engelmann spruce. The needle lengths, number of needles per unit length of twig, twig diameters, needle weights, and twig weights were determined for about 10 twig segments for each species. The weight/drag ratios (or $\rho D/C_D$) of the composite structures were calculated using average values for the variables needed. Using these data in the particle height-vs-time formulas (appendix D) resulted in initial particle heights that were too great to allow the twig to return to the ground before burning out, for all the examples tried. In other words, no spot distance advantage was found for the composite firebrands. This does not mean that all combinations of twig diameter, needle length, number of needles per unit of twig length, etc., would not go farther than a stem segment. But, for the species sampled, the necessary combination was not found. No further effort was spent on "two stage" firebrand structures.

The structure of the wind field that carries the burning brand has a powerful influence on the distance it travels. For flight over forested flat terrain a simple logarithmic variation of velocity with height suffices for a windspeed model. Using the profile shown in figure 1, the path of the burning brand is readily computed. In this computation the logarithmic profile of windspeed with height is extended below treetop height to zero velocity. A maximum distance would be predicted by assuming the windspeed below treetop height to be constant. At the other extreme, one might consider the crown layer to be impenetrable by a firebrand and set the velocity to zero. Neither extreme is realistic, but the extended logarithmic profile interpolates between them, so is used for convenience.

For wind over uneven terrain--e.g., blowing across a ridge-valley system--it is necessary to model the variation of windspeed with horizontal distance (fig. 2) and to include the vertical wind component as well. The crude model developed in appendix E includes these variations, but omits some well established features of such a wind field:

1. The variation of windspeed and direction with height commonly called the Ekman spiral (see, e.g., Brown 1974) is not included in the model. An isobar at constant height is used in the model as a "lid" on the flow beneath it, as done by Fosberg and others (1976) and friction is ignored down to a thin layer close to the surface. In this surface friction layer the logarithmic profile used in the flat terrain model is employed, with a characteristic horizontal velocity that depends on local terrain height.

2. The "rotor" or recirculation flow often observed on the lee side of a ridge (Schroeder and Buck 1970) is not included in the wind model. There exist mathematical models of windflow over terrain features that include "rotor" and "lee wave" effects (Alaka 1960) but they are complex and demand more data than just the terrain profile. Trial use of the simplified wind model presented here will reveal whether or not the simplification has degraded its accuracy beyond utility in rough terrain.

3. The friction length scale of the flow in the friction layer is treated as a constant in this model. Its value is set to 0.1313 times the average treetop height, based upon measured data in relatively flat terrain with a uniform forest cover (Tanner and Pelton 1960; Marunich 1975). This may prove to be a weak point in the velocity profile model because uniform forest cover over nonuniform terrain with significant elevation change is not the usual case. The user is asked to select an "average" canopy top height when assessing maximum spotting distance, but no guidance is given for determining the appropriate average when forest cover and open areas must both be considered.

Determination of the trajectory of the firebrand particle carried by the model flow fields is straightforward. Although some approximations are made in the analyses, each can be justified quantitatively. It is felt that the approximations and model uncertainties in the burning rate and wind field descriptions dominate errors introduced in calculating the flight of the particle. The lofting phase of the trajectory (appendix E) is treated less precisely than the transport phase (appendix F) but in neither case should the integration of the equations of motion introduce error as large as the uncertainties in the models on which they are based.

PUBLICATIONS CITED

Alaka, M. A.
1960. The airflow over mountains. World Meteorol. Organ. Tech. Note 34, 135 p. (WMO-No. 98, TP. 43), Geneva, Switz.

Anderson, Hal E.
1969. Heat transfer and fire spread. USDA For. Serv. Res. Pap. INT-69, 20 p., Intermt. For. and Range Exp. Stn., Ogden, Utah

Barrows, J. S.
1951. Fire behavior in northern Rocky Mountain Forests. USDA For. Serv. North. Rocky Mt. For. and Range Exp. Stn. Pap. 29, 103 p.

Baskerville, G. L.
1965A. Dry-matter production in immature balsam fir stands. For. Sci. Monogr. 9, 42 p.

Baskerville, G. L.
1965B. Estimation of dry weight of tree components and total standing crop in conifer stands. Ecology 46:867-869.

Baynton, H. W.
1965. Wind structure in and above a tropical forest. J. Appl. Meteorol. 4(6):670-675.

Bergen, J. D.
1971. Vertical profiles of windspeed in a pine stand. For. Sci. 17(3):314-321.

Brown, James K.
1965. Estimating crown fuel weights of red pine and jack pine. USDA For. Serv. Res. Pap. LS-20, 12 p. Lake States For. Exp. Stn., St. Paul, Minn.

Brown, James K.
1977. Weight and density of crowns of Rocky Mountain conifers. USDA For. Serv. Res. Pap. INT-197, 56 p.

Brown, James K., J. A. Kendall Snell, and David L. Bunnell.
1977. Handbook for predicting slash weight of western conifers. USDA For. Serv. Gen. Tech. Rep. INT-37, 35 p. Intermt. For. and Range Exp. Stn., Ogden, Utah.

Brown, R. A.
1974. Analytical methods in planetary boundary--layer modelling. 148 p. Halsted Press (John Wiley & Sons) New York.

Clark, Alexander III, and Michael A. Taras.
1976. Biomass of shortleaf pine in a natural sawtimber stand in northern Mississippi. USDA For. Serv. Res. Pap. SE-146, 32 p. Southeast. For. Exp. Stn., Asheville, N.C.

Clements, Hubert B.
1977. Liftoff of forest firebrands. USDA For. Serv. Res. Pap. SE-159, 11 p. Southeast. For. Exp. Stn., Asheville, N.C.

Florida Division of Forestry
1973. Forest fire suppression tactics, a training manual. Florida Dep. Agric. and Consum. Serv., Div. For., 41 p.

Fons, Wallace L.
1940. Influence of forest cover on wind velocity. J. For. 38(6):481-486.

Fosberg, Michael A., William E. Marlatt, and Lawrence Krupnak.
1976. Estimating airflow patterns over complex terrain. USDA For. Serv. Res. Pap. RM-162, 16 p. Rocky Mt. For. and Range Exp. Stn., Fort Collins, Colo.

Gisborne, H. T.
1936. Measuring fire weather and forest inflammability. U. S. Dep. Agric. Circ. 398.

Gisborne, H. T.
1941. How the wind blows in the forests of northern Idaho. USDA For. Serv., Div. For. Prot. North. Rocky Mt. For. and Range Exp. Stn., 12 p. North. For. Fire Lab., Missoula, Mont.

Johansen, Ragnar W., and W. Henry McNab.
1977. Estimating logging residue weights from standing slash pine for prescribed burns. South. J. Appl. For. 1(2):1-6.
Kanury, A. Murty.
1974. Mass regression in the pyrolysis of pine wood macrocylinders in a nitrogen atmosphere--an experimental study. Comb. Sci. and Tech. 9:31-36.
Keays, J. L.
1971. Complete-tree utilization. An analysis of the literature. Part II: Foliage. Forest Prod. Lab., Can. For. Serv. Dep. Fish. and For., Inf. Rep. VP-X-70, 94 p. Feb. 1971. Part IV: Crown and Slash, Inf. Rep. VP-X-77, 70 p., Mar. 1971.
Kittredge, J.
1944. Estimation of the amount of foliage of trees and stands. J. For. 42:405-412.
Kung, H. C.
1971. A mathematical model of wood pyrolysis. Factory Mutual Res. Corp. For presentation at the 1971 Spring Meeting of the West. States Sect. of the Comb. Inst., Univ. Denver, Denver, Colo.
Lee, S. L., and J. M. Hellman.
1970. Firebrand trajectory study using an empirical velocity-dependent burning law. Comb. and Flame 15:265-274.
Leonard, R. C., and C. A. Federer.
1973. Estimated and measured roughness parameters for a pine forest. J. Appl. Meteorol. 12(2):302-307.
Loomis, Robert M., Robert E. Phares, and John S. Crosby.
1966. Estimating foliage and branchwood quantities in shortleaf pine. For. Sci. 12(1):30-39.
Martin, H. C.
1971. Average winds above and within a forest. J. Appl. Meteorol. 10(6):1132-1137.
Marunich, S. V.
1975. Transactions of the State Hydrologic Institute, USSR (Trudy GGI) No. 223, p. 80-88. Translation in Soviet Hydrology: Selected Papers, No. 2, p. 51-54.
Morton, B. R.
1965. Modeling fire plumes. *In* Proc. Tenth Symp. (International) on Combustion, p. 973-982. The Comb. Inst., Pittsburgh, Pa.
Muraszew, A., and J. B. Fedele.
1976. Statistical model for spot fire hazard. Aerospace Rep. 77(7588)-1, 109 p. The Aerospace Corp., El Segundo, Calif.
Muraszew, A., J. B. Fedele, and W. C. Kuby.
1975. Firebrand investigation. Aerospace Rep. ATR-75(7470)-1, 104 p. The Aerospace Corp., El Segundo, Calif.
Nielsen, H. J., and L. N. Tao.
1965. The fire plume above a large free-burning fire. *In* Proc. Tenth Symp. (International) on Combustion, p. 965-972. The Comb. Inst., Pittsburgh, Pa.
Oliver, H. R.
1971. Wind profiles in and above a forest canopy. Royal Meteorol. Soc. 97:548-553.
Ovington, J. D., and H. A. I. Madgwick.
1959. Distribution of organic matter and plant nutrients in a plantation of Scots Pine. For. Sci. 5:344-355.
Putnam, A. A., and C. F. Speich.
1963. A model study of the interaction of multiple turbulent diffusion flames. *In* Proc. Ninth Symp. (International) on Combustion, p. 867-877. The Comb. Inst., Pittsburgh, Pa.
Putnam, Abbott A.
1965. A model study of wind-blown free-burning fires. *In* Proc. Tenth Symp. (International) on Combustion, p. 1039-1046. The Comb. Inst., Pittsburgh, Pa.

Rasbash, D. J., Z. W. Rogowski, and G. W. Stark.
1956. J. Inst. Fuel 35:94.
Raynor, G. S.
1971. Wind and temperature structure in a coniferous forest and a contiguous field. For. Sci. 17(3):351-363.
Rogerson, T. L.
1964. Estimating foliage on loblolly pine. USDA For. Serv. Res. Note SO-16, 3 p. South. For. Exp. Stn., New Orleans, La.
Ryan, Bill C.
1977. A mathematical model for diagnosis and prediction of surface winds in mountainous terrain. J. Appl. Meteorol. 16(6):571-584.
Schroeder, Mark J., and Charles C. Buck.
1970. Fire weather...a guide for application of meteorological information to forest fire control operations. USDA For. Serv. Agric. Handb. 360, 229 p. Gov. Print. Off., Washington, D.C.
Steward, F. R.
1964. Linear flame heights for various fuels. Comb. and Flame 8:171-178.
Sutton, O. G.
1953. Micrometeorology. 333 p. McGraw-Hill Book Co., New York.
Tanner, C. B., and W. L. Pelton.
1960. Potential evapotranspiration estimates by the approximate energy balance of Penman. J. Geophys. Res. 65:3391-3413.
Taras, Michael A., and Alexander Clark III.
1975. Aboveground biomass of loblolly pine in a natural, uneven-aged sawtimber stand in central Alabama. TAPPI 58(2):103-105.
Taras, Michael A., and Alexander Clark III.
1977. Aboveground biomass of longleaf pine in a natural saw-timber stand in southern Alabama. USDA For. Serv. Res. Pap. SE-162, 32 p. Southeast. For. Exp. Stn., Asheville, N.C.
Tarifa, C. Sanchez, P. Perez del Notario, and F. Garcia Moreno.
1965. On the flight paths and lifetimes of burning particles of wood. *In* Proc. Tenth Symp. (International) on Combustion, p. 1021-1037. The Comb. Inst., Pittsburgh, Pa.
Tarifa, Carlos Sanchez, Pedro Perez del Notario, Francisco Garcia Moreno, and Antonio Rodriguez Villa.
1967. Transport and combustion of firebrands. Final Rep. FG-SP-146 (Vol II), 90 p. Madrid, Spain (report to USDA For. Serv.).
Thomas, P. H.
1963. The size of flames from natural fires. *In* Proc. Ninth Symp. (International) on Combustion, p. 844-859. The Comb. Inst., Pittsburgh, Pa.
Thomas, P. H., R. Baldwin, and J. M. Heselden.
1965. Buoyant diffusion flames: some measurements of air entertainment, heat transfer, and flame merging. *In* Proc. Tenth Symp. (International) on Combustion, p. 983-996. The Comb. Inst., Pittsburgh, Pa.
Turner, J. S.
1973. Buoyancy effects in fluids. 367 p. Cambridge University Press.
USDA Forest Service.
1956. Glossary of terms used in forest fire control. Agric. Handb. 104, 24 p. Gov. Print. Off., Washington, D.C.
USDA Forest Service, Northern Region.
1973. Fuel management planning and treatment guide--prescribed burning guide, Region 1. USDA For. Serv. pamphlet (5150), 56 p. North. Reg., Missoula, Mont.
VanWagner, C. E.
1977. Conditions for the start and spread of crown fire. Can. J. For. Res. 7:23-34.
Wade, Dale D.
1969. Estimating slash quantity from standing loblolly pine. USDA For. Serv. Res. Note SE-125, 4 p. Southeast. For. Exp. Stn., Asheville, N.C.

Weetman, G. F., and R. Harland.
1964. Foliage and wood production in unthinned black spruce in northern Quebec. For. Sci. 10(1):80-88.
Wendel, G. W.
1960. Fuel weights of pond pine crowns. USDA For. Serv. Res. Note 149, 2 p. Southeast. For. Exp. Stn., Asheville, N.C.
Whittaker, R. H., Neil Cohen, and Jerry S. Olsen.
1963. Net production relations of three tree species at Oak Ridge, Tennessee. Ecology 44(4):806-809.
Wohl, Kurt, Carl Gazley, and Numer Kapp.
1949. Diffusion flames. *In* Proc. Third Symp. on Combustion Flame, and Expl. Phenomena. 288-300. Williams and Wilkins Co., Baltimore, Md.

APPENDIX A: FLAME STRUCTURE MODEL

In this appendix a simple phenomenological model is presented for the structure of a large flame burning in still air. Approximate expressions are developed for the mean length (height) of the flame, the velocity of the gas flow within the flame, and the dynamic pressure profile. To derive these expressions a model of such a flame is postulated and analyzed. Although the model is obviously over-simplified and incorrect in detail, the gross relationships sought do not justify a more elaborate model. And the transparency of the model allows one to see the influence of various parameters (and assumptions) on the quantities sought.

I. *Conceptual Model*

Picture an erect right circular cone as a boundary in space. This cone marks the region within which exists gaseous fuel.[4] The fuel flows into the region axially across the circular area at the base and is consumed at the surface of the cone as it makes contact with the air. The tip of the cone is the tip of the flame. The cone of fuel gas is surrounded by a cylindrical sheath of varying radius within which flow the products of combustion plus entrained ambient air. In this annular sheath the gas flows upward, as does the fuel gas. Outside this sheath, ambient air flows radially inward toward the vertical axis of the flame. The following symbols will be used to describe the flows and boundaries discussed:

Symbols

ρ = gas density (mass/unit volume)
r = radial distance from central axis
z = vertical distance from base of flame
u = inward radial velocity
w = upward axial velocity
ϕ = mean mass ratio of air to fuel producing flame-product/air mix
η = entrainment velocity ratio (u/w), a constant with height by assumption
g = acceleration of gravity

Subscripts

f refers to fuel gas (condition or boundary location)
a refers to ambient air (condition or boundary location)
p refers to products of reaction (plus admixed air)
o refers to conditions at the base of the flame
F refers to conditions at the tip of the flame

[4] The gaseous fuel consists of the products of volatilization and pyrolysis of the solid fuel being burned, plus some combustion products and some poorly mixed air. In this simplified model the mixture is idealized as pure gaseous fuel.

II. *Mathematical Model*

Using these symbols we can write the conservation equations of the gross flame structure. The entrainment assumption (Thomas 1963; Thomas and others 1965; Turner 1973) is made here in the form:

$$u = \eta w \tag{A1}$$

and w is assumed to be a function of z only. The conservation of mass and momentum are readily expressed in terms of an intermediate variable, m, representing the mass in a unit height of the entire flame structure, divided by π:

$$m = \rho_p\left(r_a^2 - r_f^2\right) + \rho_f r_f^2. \tag{A2}$$

The conservation of mass relationship is then:

$$\frac{d}{dz}(mw) = 2\rho_a r_a u. \tag{A3}$$

The air/fuel ratio involved in forming the "product" gas (not chemical stoichiometry) is specified by the parameter ϕ. Holding ϕ constant leads to:

$$mw + \phi\rho_f w r_f^2 = (1 + \phi)(\rho_f w r_f^2)_o. \tag{A4}$$

The conservation of momentum, including the effects of buoyancy and "drag" due to air entrainment is expressed by:

$$mw\frac{dw}{dz} = g(r_a^2\rho_a - m) - 2\rho_a r_a uw. \tag{A5}$$

These equations are essentially the same as those used by others (Steward 1964; Morton 1965; Nielsen and Tao 1965) in models of flame size.

Using equations (A2) and (A4) one can derive the following useful intermediate relationship:

$$w r_a^2 = \left\{\frac{\rho_f}{\rho_p}\left(\frac{1 + \phi}{\phi}\right) - \frac{1}{\phi}\right\}\frac{mw}{\rho_f} - \left(\frac{1 + \phi}{\phi}\right)\left(\frac{\rho_f}{\rho_p} - 1\right)(w r_f^2)_o. \tag{A6}$$

Here it has also been assumed that the inner core of fuel is at constant density:

$$\rho_f = (\rho_f)_o. \tag{A7}$$

Using equation (A6) in equation (A5) multiplied through by w gives:

$$mw^2\frac{dw}{dz} = \rho_a g\left\{\frac{mw}{\rho_f}\left(\frac{\rho_f}{\rho_p}\left(\frac{1 + \phi}{\phi}\right) - \frac{1}{\phi}\right) - \left(\frac{1 + \phi}{\phi}\right)\left(\frac{\rho_f}{\rho_p} - 1\right)(w r_f^2)_o\right\} - mwg - 2\rho_a r_a uw^2. \tag{A8}$$

In a shorthand form this can be written as

$$w\frac{d}{dz}(mw^2) = g(\alpha mw - \beta(mw)_o) \tag{A9}$$

where α and β are constants given by:

$$\alpha = \left(\frac{1 + \phi}{\phi}\right)\frac{\rho_a}{\rho_p} - \frac{1}{\phi}\frac{\rho_a}{\rho_f} - 1 \tag{A10}$$

$$\beta = \left(\frac{1 + \phi}{\phi}\right)\frac{\rho_a}{\rho_f}\left(\frac{\rho_f}{\rho_p} - 1\right). \tag{A11}$$

Note that the mass conservation and entrainment equations combined can be written as:

$$\begin{aligned}\frac{d}{dz}(mw) &= 2\eta\rho_a r_a w = 2\eta\rho_a w^{1/2}(wr_a^2)^{1/2} \\ &= 2\eta\rho_a w^{1/2}\left\{\frac{\alpha + 1}{\rho_a}mw - \frac{\beta}{\rho_a}(mw)_o\right\}^{1/2} \\ &= 2\eta\left\{\rho_a w\left((\alpha + 1)mw - \beta(mw)_o\right)\right\}^{1/2}\end{aligned} \tag{A12}$$

or

$$m^{1/2}\frac{d}{dz}(mw) = 2\eta\left\{(mw)\rho_a\left((\alpha + 1)mw - \beta(mw)_o\right)\right\}^{1/2}. \tag{A13}$$

Multiplying (A9) through by (mw) makes the left hand side a perfect differential:

$$\frac{d}{dz}\left((mw^2)^2\right) = 2gmw\left(\alpha mw - \beta(mw)_o\right). \tag{A14}$$

Equations (A13) and (A14) are now further simplified by noting that, over most of the length of the flame,

$$\alpha mw >> \beta(mw)_o, \tag{A15}$$

an inequality that arises from the large ratio of air to fuel noted for natural fires (Thomas 1963). By eliminating the second term from the righthand side of (A13) and (A14) one arrives at[5]

$$m^{1/2}\frac{d}{dz}(mw) \doteq 2\eta\left((\alpha + 1)\rho_a\right)^{1/2}mw \tag{A16}$$

$$\frac{d}{dz}\left((mw^2)^2\right) \doteq 2\alpha g(mw)^2. \tag{A17}$$

Substituting the expressions:

$$P = mw; \qquad Q = mw^2 \tag{A18}$$

into these equations gives:

---

[5]Actually, it is not necessary to make this approximation to proceed with the analysis, but the difference resulting is minor and therefore not justifiable in view of the level of accuracy of this model.

$$(P/Q^{1/2})\frac{dP}{dz} = 2\eta\left((\alpha + 1)\rho_a\right)^{1/2}P \tag{A19}$$

$$\frac{dQ^2}{dz} = 2\alpha g P^2 \tag{A20}$$

or

$$\frac{dP}{dz} = 2\eta\left((\alpha + 1)\rho_a\right)^{1/2}Q^{1/2} \tag{A21}$$

$$\frac{dQ}{dz} = \alpha g P^2/Q. \tag{A22}$$

Dividing one equation by the other gives:

$$\frac{dP}{dQ} = \frac{2\eta}{\alpha g}\left((\alpha + 1)\rho_a\right)^{1/2}Q^{3/2}/P^2 \tag{A23}$$

or

$$\frac{2}{5}Q^{5/2} - \frac{\alpha g}{2\eta}\frac{\frac{1}{3}P^3}{\left((\alpha + 1)\rho_a\right)^{1/2}} = \text{constant} = \frac{2}{5}S \tag{A24}$$

$$Q^{1/2} = \left\{S + \frac{5}{12}\frac{\alpha g P^3}{\eta\left((\alpha + 1)\rho_a\right)^{1/2}}\right\}^{1/5}. \tag{A25}$$

III. *Flame Length*

This last expression can be used directly in equation (A21) to provide a formula for flame length. Note that

$$\frac{dP}{dz} = 2\eta\left((\alpha + 1)\rho_a\right)^{1/2}\left\{S + \frac{5}{12}\frac{\alpha g}{\eta\left((\alpha + 1)\rho_a\right)^{1/2}}P^3\right\}^{1/5}. \tag{A26}$$

Evaluating the constant S at the base of the flame gives:

$$S = (mw^2)_o^{5/2} - \frac{5\alpha g}{12\eta}\frac{(mw)_o^3}{\left((\alpha + 1)\rho_a\right)^{1/2}} \tag{A27}$$

so that (A26) can be written in terms of P normalized by its value at the flame base, P_o, in the form

$$\frac{d(P/P_o)}{\left\{1 + \frac{5}{12}\frac{\alpha g}{\eta\left((\alpha + 1)\rho_a\right)^{1/2}}\frac{m_o^{1/2}}{w_o^2}\left(\left(\frac{P}{P_o}\right)^3 - 1\right)\right\}^{1/5}} = \frac{2\eta\left((\alpha + 1)\rho_a\right)^{1/2}}{m_o^{1/2}}\,dz. \tag{A28}$$

Now, since

$$(P/P_o)\big|_{z=z_F} = P_F/P_o = 1 + \phi, \tag{A29}$$

the flame length formula is:

$$2\eta\left(\frac{\rho_a(\alpha + 1)}{m_o}\right)^{1/2} z_F = \int_1^{1+\phi} \left\{1 + \frac{5}{12} \frac{\alpha g}{\eta\left((\alpha + 1)\rho_a\right)^{1/2}} \frac{m_o^{1/2}}{w_o^2}(x^3 - 1)\right\}^{-1/5} dx. \tag{A30}$$

The second term in the radical in the integrand is much larger than unity over most of the length of the flame so that, to a level of approximation consistent with this analysis we have:

$$2\eta\left(\frac{\rho_a(\alpha + 1)}{m_o}\right)^{1/2} z_F \doteq \left\{\frac{12}{5} \frac{\eta\left(\rho_a(\alpha + 1)\right)^{1/2} w_o^2}{\alpha g m_o^{1/2}}\right\}^{1/5} \int_1^{1+\phi} x^{-3/5} dx$$

$$\doteq \left\{\frac{12}{5} \frac{\eta\left(\rho_a(\alpha + 1)\right)^{1/2} w_o^2}{\alpha g m_o^{1/2}}\right\}^{1/5} \frac{5}{2}\left((1 + \phi)^{2/5} - 1\right). \tag{A31}$$

This result is very similar to that obtained by Steward (1964) and exhibits the power law found by other investigators (Wohl and others 1949; Putnam and Speich 1963; Putnam 1965).

Thomas (1963) presents experimental data in dimensionless form, with which this formula can be compared. In the notation used here, his dimensionless form can be written as

$$z_F/2(r_a)_o = K\left\{(\rho_f w)_o/\left(\rho_a(2r_{a,o}g)^{1/2}\right)\right\}^N \tag{A32}$$

where K and N are empirical constants. Noting that

$$m_o = (\rho_f r_f^2)_o = (\rho_f r_a^2)_o, \tag{A33}$$

equation (A31) can be cast in the form of (A32), with the result:

$$N = \frac{2}{5} \tag{A34}$$

$$K = \frac{5}{2}\left(\frac{24}{5}\right)^{1/5}\left(\frac{\eta}{\alpha}\right)^{1/5} \frac{(1 + \phi)^{2/5} - 1}{4\eta(\alpha + 1)^{2/5}}. \tag{A35}$$

The numerical value of K for natural fires is to be estimated by using appropriate values for ϕ, η, and the density ratios appearing in the parameter α. Typical values might be (Thomas 1963)

$$\rho_a/\rho_p = 8/3; \quad \rho_a/\rho_f = 5/3; \quad \phi = 30; \quad \eta = 0.075. \tag{A36}$$

Using these values we find

$$K = 12.4 \tag{A37}$$

which value is about half of that reported by Thomas (1963) for the experiments of Putnam and Speich (1963) using city gas, adjusted for the ratio of heat content of wood volatiles to that of methane. The exponent (N) of 2/5 is the dimensionally correct value and is a good correlation value for the data of Putnam and Speich, although Thomas reports better agreement with a variety of wood crib data using an exponent of 0.61. Note that if one replaces the lower limit of the integral in equation (A31) with zero--amounting to complete neglect of the fuel gas flow at the base of the flame with respect to the flow of product gas at the tip --the equation for the flame length becomes

$$z_F/2(r_a)_o = 16\left\{(\rho_f w)_o/\rho_a(2gr_{a,o})^{1/2}\right\}^{2/5} \tag{A38}$$

using the constants given in (A36) above. This expression gives a better fit than K = 12.4 to the experimental data given in Thomas' survey, and will be used in this paper.

IV. *Gas Velocity and Dynamic Pressure*

The mean gas velocity within the flame can be expressed in terms of the distance from the flame base, using the expressions developed above. From (A25) and (A27) we can write (w/w_o) in terms of (P/P_o), since Q is wP:

$$w/w_o = Q/w_o P = \left\{(mw^2)_o^{5/2} + \frac{5}{12}\frac{\alpha g}{\eta}\frac{(mw)_o^3}{(\rho_a(\alpha+1))^{1/2}}\left(\left(\frac{P}{P_o}\right)^3 - 1\right)\right\}^{2/5} \Big/ (w_o P). \tag{A39}$$

Again neglecting the smaller terms in the radical this can be approximated by:

$$w \doteq \left\{\frac{5}{12}\frac{\alpha g}{\eta}\frac{P_o^{1/2}}{((\alpha+1)\rho_a)^{1/2}}\right\}^{2/5}\left(\frac{P}{P_o}\right)^{1/5}. \tag{A40}$$

The dependence of (P/P_o) on z is readily obtained from (A31) by replacing z_F by z and $(1+\phi)$ by (P/P_o). So doing leads to the form:

$$w \doteq \left\{\frac{5}{12}\frac{\alpha g}{\eta}\frac{P_o^{1/2}}{((\alpha+1)\rho_a)^{1/2}}\right\}^{2/5}\left\{1 + \frac{4\eta}{5}\left(\frac{\rho_a(\alpha+1)}{m_o}\right)^{1/2}\left(\frac{5}{12}\frac{\alpha g}{\eta w_o^2}\left(\frac{m_o}{\rho_a(\alpha+1)}\right)^{1/2}\right)^{1/5} z\right\}^{1/2}. \tag{A41}$$

This expression simplifies also, since we are concerned only with the upper part of the flame, where the second term in the radical on the righthand side is much greater than unity. Neglecting the one leads to considerable cancellation of factors:

$$w \doteq (\alpha g z/3)^{1/2}. \tag{A42}$$

The value of α, from (A10), is very nearly

$$\alpha \doteq \rho_a/\rho_p - 1 \tag{A43}$$

since ϕ is about 30. This leads to the form:

$$w \doteq 0.408\left(2g(\rho_a/\rho_p - 1)z\right)^{1/2}. \tag{A44}$$

The only difference between this expression and the empirical equation given in Thomas (1963), based on experimental work by Rasbash and others (1956) with liquid fuel fires, is the numerical factor. Thomas reports a coefficient of 0.36, or 12 percent less than the value here. The difference is no doubt due to the gross nature of this model.

The mean density within the flame structure is needed to describe the dynamic pressure profile. Average density ($\bar{\rho}$) is readily derivable from the variables already used; since by definition of average

$$\bar{\rho} = m/r_a^2 = mw/(wr_a^2) = P/(wr_a^2). \tag{A45}$$

From (A2), (A6), (A7), and (A10) we have

$$wr_a^2 = \frac{\alpha + 1}{\rho_a} P - \beta \frac{P_o}{\rho_a} \tag{A46}$$

so that

$$\bar{\rho}/\rho_a = P\left((\alpha + 1)P - \beta P_o\right)^{-1} = \left((\alpha + 1) - \beta P_o/P\right)^{-1}. \tag{A47}$$

This expression simplifies by referring the mean density to the value at the tip of the flame and using the scaling law for the parameter P referred to its value at the flame tip:

$$P/P_F \doteq (z/z_F)^{5/2}; \quad P \doteq (1 + \phi)P_o(z/z_F)^{5/2}. \tag{A48}$$

Using this form and noting that $\bar{\rho}$ at the flame tip is ρ_p, equation (A47) can be approximated for the upper part of the flame by:

$$\bar{\rho}/\rho_p \doteq \left(1 + (1 - \rho_p/\rho_f)(1 - (z_F/z)^{5/2})/\phi\right)^{-1}. \tag{A49}$$

From this form it is apparent that, over most of the upper part of the flame, the density can be considered constant and equal to the flame tip value.

The dynamic pressure, referred to its value at the tip of the flame is quickly derived now:

$$\bar{\rho}w^2/\rho_p w_F^2 = \frac{\bar{\rho}}{\rho_p}\left(\frac{w}{w_F}\right)^2 = \left(\frac{z}{z_F}\right)\Big/\left(1 - \frac{(1 - \rho_p/\rho_f)}{\phi}\left(\left(\frac{z_F}{z}\right)^{5/2} - 1\right)\right). \tag{A50}$$

V. *Formulae Used in Firebrand Lofting Analysis*

The formulae derived above can be cast in practical form for use in the firebrand lofting computations. Equation (A38) gives the flame height, but in terms difficult to apply. It can be simplified if one observes that the rate of fuel consumption (mass per unit time, $\dot{M}$) can be written as:

$$\dot{M} = \pi\rho_f(r_a^2 w)_o. \tag{A51}$$

Inserting this into (A38) and canceling out $(r_a)_o$ gives

$$z_F \doteq 16(4/\pi\rho_a g^{1/2})^{2/5}(\dot{M})^{2/5}. \tag{A52}$$

Assuming approximately standard atmospheric conditions

$$\rho_a = 0.075 \text{ lb/ft}^3 = 1.2 \text{ kg/m}^3 \tag{A53}$$

$$g = 32 \text{ ft/s}^2 = 9.8 \text{ m/s}^2 \tag{A54}$$

so

$$z_F = 25(\dot{M})^{2/5} \tag{A55}$$

where the flame height is in feet and the fuel consumption rate is in pounds mass per second, or

$$z_F = 10.4(\dot{M})^{2/5} \tag{A56}$$

if the units are meters and kilograms per second. Figure A-1 compares predicted flame heights, using this equation, to values observed in the burning of wood cribs. The data were transcribed graphically from figures presented by Thomas (1963). The agreement between the predicted heights and observed heights is quite satisfactory, but application of the equation to burning trees involves extrapolation beyond the range shown in figure A-1.

For velocity all one needs to do is express the value at height z as a function of the flame tip value

$$w/w_F = (z/z_F)^{1/2}. \tag{A57}$$

and calculate w_F from (A44). Here we assume that the density ratio ρ_a/ρ_p is 8/3, as before,[6] to obtain

[6] In other words, the flame edge is defined as the 500 C outline, about the limit of carbon particle visibility, and the product gas molecular weight is essentially that of air.

$$w_F = \begin{cases} 4.2 z_F^{1/2} & \text{ft/s}, \quad z_F \text{ in ft} \\ 2.3 z_F^{1/2} & \text{m/s}, \quad z_F \text{ in m.} \end{cases} \tag{A58}$$

The peak dynamic pressure in the flame occurs at the flame tip in this model, and the value would be given by q_F, where

$$q_F = \frac{1}{2} \rho_p w_F^2 = \frac{1}{6} \rho_a g z_F (1 - \rho_p/\rho_a) \tag{A59}$$

or

$$q_F = \begin{cases} 0.0078\ z_F & \text{lbf/ft}^2, \quad z_F \text{ in ft} \\ 1.23\ z_F & \text{N/m}^2, \quad z_F \text{ in m.} \end{cases} \tag{A60}$$

For all practical purposes the dynamic pressure can be considered to increase linearly with height.

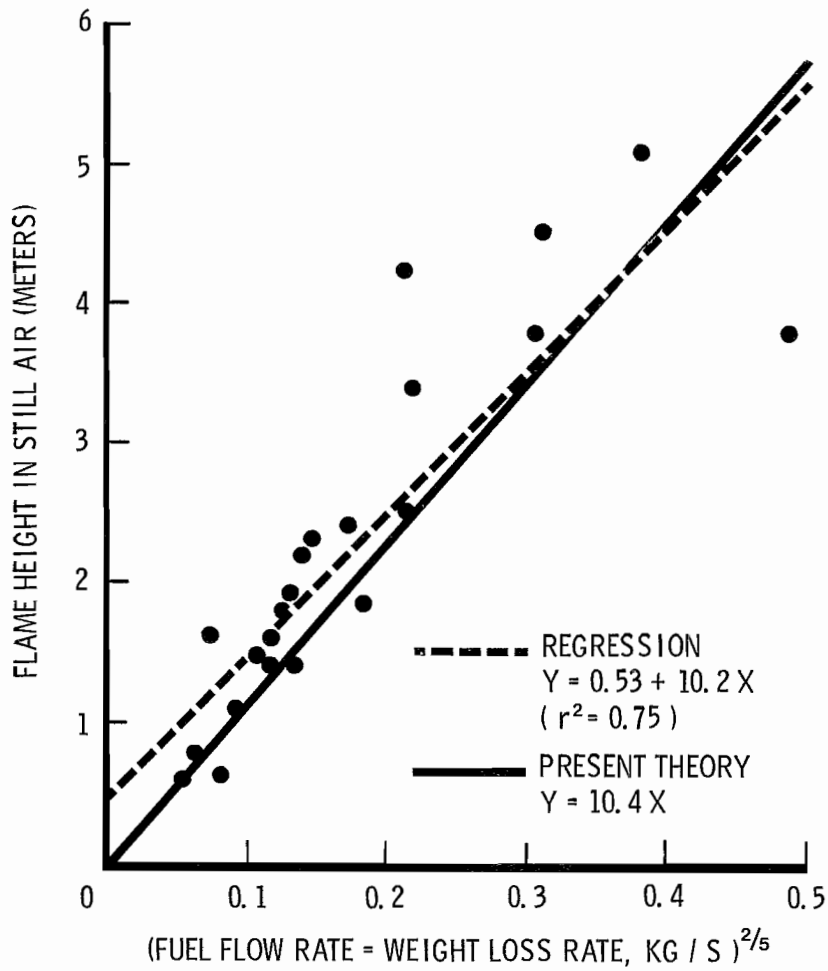

Figure A-1.--Comparison of data on flame heights (Laboratory Wood Crib Burns, Thomas 1963) with predictions from present theory.

APPENDIX B: THE BUOYANT PLUME ABOVE A STEADY FLAME

The vertical transport of a firebrand into the prevailing windstream may include a period of flight in the buoyant plume flow above the flame from which it came. This "lofting" phase can be approximated by an upper-limit calculation, as discussed in the text. To perform the trajectory calculations it is necessary to describe the fluid flow field in the buoyant plume. From the tip of the (transient) flame upward we use here the scaling laws for a fully-developed turbulent buoyant plume in still air.

The decay of velocity in a buoyant plume occurs through accretion of ambient air into the flow. In still air this process is usually represented by an "entrainment parameter" as used in appendix A, giving the ratio of inflow velocity to vertical velocity. The entrainment parameter is of the order of 0.1, so use of a "still air" model clearly gives an upper limit to the firebrand-lofting capability of the plume. A plume in a shearing wind environment would be eroded more rapidly with height.

The fact that the plume is treated as fully developed (that is, steady rather than changing with time) is probably not as conservative as it may seem. This is so because prior to the "torching" of the tree or trees that produce the plume, a substantial fire must have burned in the same place for a considerable period of time. This fire will have established a convection plume that is then merely amplified by the heat pulse from the burning tree crown(s).

Well-accepted analysis of a free buoyant plume (Turner 1973) provides the scaling laws needed. The simplest applicable model is one that describes the self-similar flow field for constant buoyant flux. Let

b = mean radius of plume
G = buoyancy = $g(1 - \bar{\rho}/\rho_a)$
$\bar{w}$ = mean vertical velocity
F = buoyant flux = $\bar{w}b^2G$ = constant

where

g = acceleration of gravity
$\bar{\rho}$ = mean density in the plume
ρ_a = ambient air density.

The scaling laws of interest are (Turner 1973)

$$b = \frac{6}{5}\eta z \tag{B1}$$

$$\bar{w} = \frac{5}{6\eta}\left(\frac{9}{10}\eta F\right)^{1/3} z^{-1/3} \tag{B2}$$

$$G = \frac{5F}{6\eta}\left(\frac{9}{10}\eta F\right)^{-1/3} z^{-5/3} \tag{B3}$$

where z is height and η is the entrainment parameter.

Forming ratios of these variables with their values at the tip of the flame (where $z = z_F$) we have:

$$\bar{w}/w_F = (z_F/z)^{1/3} \tag{B4}$$

$$G/G_F = (1 - \bar{\rho}/\rho_a)/(1 - \rho_P/\rho_a) = (z_F/z)^{5/3}. \tag{B5}$$

The mass density at the tip of the flame is ρ_P, as in appendix A. The density profile is given by

$$\bar{\rho}/\rho_a = 1 - (1 - \rho_P/\rho_a)(G/G_F) = 1 - (1 - \rho_P/\rho_a)(z_F/z)^{5/3} \tag{B6}$$

which leads directly to the dynamic pressure decay law:

$$q/q_F = (\bar{\rho}/\rho_P)(\bar{w}/w_F)^2 \tag{B7}$$

$$q/q_F = \left(1 - (1 - \rho_P/\rho_a)(z_F/z)^{5/3}\right)(\rho_a/\rho_P)(z_F/Z)^{2/3}. \tag{B8}$$

Using the nominal density ratio

$$\rho_P/\rho_a = 3/8 \tag{B9}$$

that was used in appendix A, equation (B8) becomes

$$q/q_F = (8/3)\left(1 - (5/8)(z_F/z)^{5/3}\right)(z_F/z)^{2/3}. \tag{B10}$$

Equation (B10) exhibits a maximum, due to the fact that the density increase rate exceeds the velocity decrease rate in the lower part of the plume. This feature assures that a firebrand particle lifted within the flame should be projected above the height of maximum dynamic pressure, which is at about 1.6 times flame height. The region between the flame tip and somewhere near this height can be thought of as a transition zone between the flame and the dissipating plume above it.

In order to express analytically the flight of a particle borne in the flame/plume flow structure it is necessary to approximate the power-law relationships given above by simpler forms. The "transition zone" concept is valuable in formulating the needed approximations. As noted in appendix A, the mean fluid density is nearly constant in the upper half of the flame, while the velocity increases as the square root of height. In the transition zone the density increases substantially while the velocity changes very little. Above the transition zone, the density again rises slowly while the velocity gradually decays. Simplified approximations, based on fitting the curve forms given in this and the previous appendix, are listed below:

$$\bar{\rho}/\rho_a = \begin{cases} 3/8 & , \quad z \leq z_F \\ (3/8)(z/z_F), & z_F < z < 1.4\ z_F \\ 0.525 & , \quad z \geq 1.4\ z_F \end{cases} \tag{B11}$$

$$\bar{w}/w_F = \begin{cases} (z/z_F)^{1/2} & , \quad z \leq z_F \\ 1 & , \quad z_F < z < 1.4\ z_F \\ (5.963/(4.563 + z/z_F))^{1/2}, & z \geq 1.4\ z_F. \end{cases} \tag{B12}$$

These simpler forms are used in the analysis of trajectories of potential firebrands. The density is underestimated by the approximate form and the velocity is overestimated, but the dynamic pressure is accurately described (fig. B-1). Overestimation of the velocity is consistent with the intent here to estimate an upper bound for spotting distance; the misestimation takes the form of a shift upward (of about 2 flame heights) of the velocity-vs-height curve.

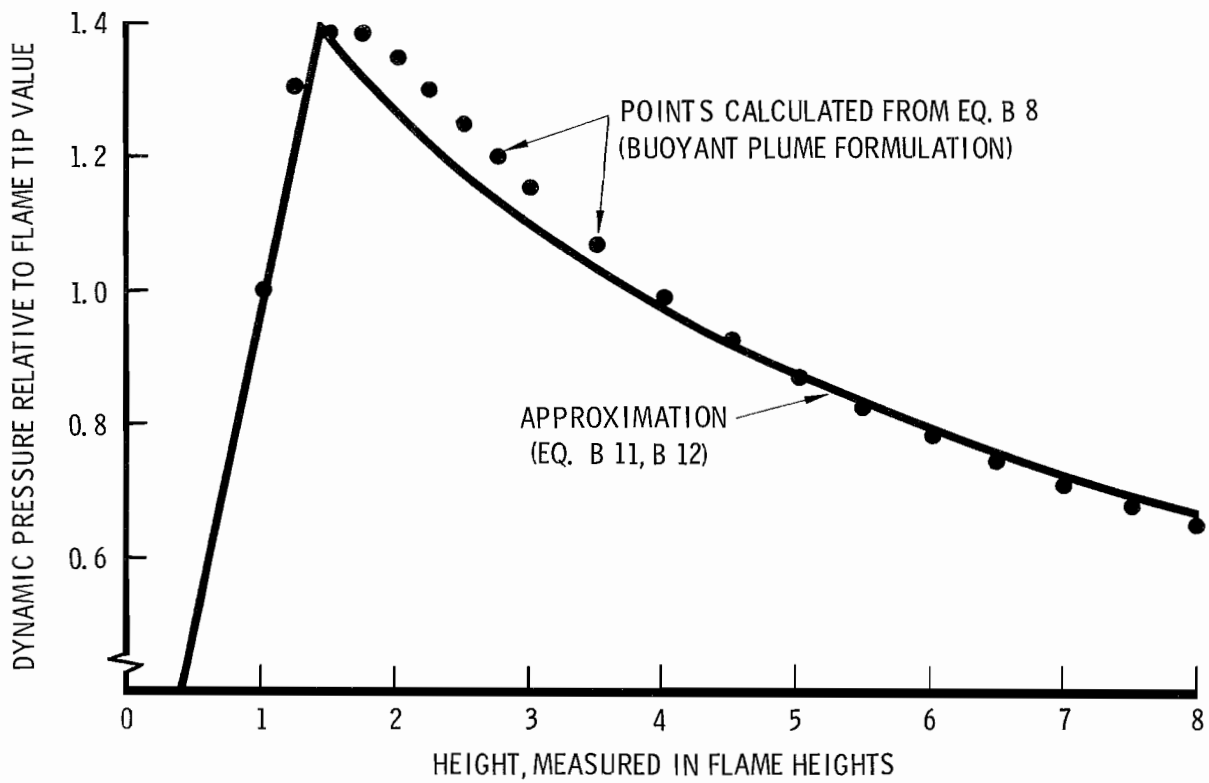

Figure B-1.--Dynamic pressure profile in and above steady flame, showing approximation used in calculating firebrand lifting ability.

APPENDIX C: FIREBRAND BURNING RATE MODEL

A firebrand burning in flight changes aerodynamic properties in at least two ways simultaneously. It loses mass and it loses volume. Woody material is pyrolyzed by heat supplied by combustion on the outer surface of the piece, and is eventually reduced totally to char. The density of char is less than that of sound or partially decayed wood, so a firebrand also loses density. By losing both density and volume, the firebrand reduces its terminal fall velocity, since that velocity is proportional to the square root of the product of density and linear dimension in the direction of relative wind (Tarifa and others 1965).

We are dealing with relatively small, light objects as firebrands here so terminal fall velocity is achieved in a short distance. The subsequent flight of the object is dictated by the changes in terminal velocity over time (or distance). Thus the simplest model one might construct to represent the burning of firebrands in flight would be one that allowed the prediction of terminal fall velocity directly. This fact was recognized by Tarifa and others (1967). The final product of that investigation was a correlation of terminal velocity with a complicated variable that is linear in time. The correlation curve is roughly bell-shaped.

The data reported in these earlier investigations dealt with various object shapes (plates, cylinders, and spheres) of differing sizes and made from different woods. These objects do not necessarily typify naturally occurring potential firebrands, but the fact that they all yielded a similar behavior pattern encourages the use of a "universal" burning rate law.

Data taken at the Northern Forest Fire Laboratory[7] on limbwood sections with bark cover were used to develop the model used in this analysis. The burning rate law is postulated from dimensional considerations and can be derived as follows. Let

M = mass of burning particle
ρ_s = mean density of particle
D = dimension of particle in direction of relative wind
(= thickness of plate, diameter of cylinder or sphere)
A = cross-sectional area presented to wind by particle
U = velocity of wind over particle
ρ_a = density of air.

[7]Data reported by Muraszew and others (1975).

The rate of mass loss is supposed to be proportional to the rate of supply of air to the surface (Lee and Hellman 1970);

$$\frac{dM}{dt} = -K_1 \rho_a A U \tag{C1}$$

where K_1 is a dimensionless constant. Since

$$M = C \rho_s A D \tag{C2}$$

where C is a geometrical constant fixed by the shape of the particle, equation (C1) can be written as

$$A \frac{d}{dt}(\rho_s D) + \rho_s D \frac{dA}{dt} = - \frac{K_1}{C} \rho_a A U. \tag{C3}$$

The data on limbwood sections (table C-1) showed the fractional decrease in A usually to be much less than the fractional decrease in M over most of the life-time of burning brands,[8] so to a fair approximation one might neglect the second term on the left-hand side of (C3) and obtain

$$\frac{d}{dt}(\rho_s D) \doteq \frac{K_1}{C} \rho_a U = -K \rho_a U. \tag{C4}$$

For constant windspeed, such as in the wind tunnel tests, equation (C4) can be integrated to give:

$$(\rho_s D)/(\rho_s D)_o = 1 - K \rho_a U t/(\rho_s D)_o \tag{C5}$$

where the subscript o indicates the initial value of the parameter. This is the form that was used to estimate a value for the constant K. A constrained linear regression of the form

$$y = bx \tag{C6}$$

with

$$y = 1 - (\rho_s D)/(\rho_s D)_o \tag{C7}$$

$$x = \rho_a U t/(\rho_s D)_o \tag{C8}$$

was performed on the data from 33 tests on ovendried limbwood sections. The variable y was established by using

$$y = 1 - \left((\rho_s M)/(\rho_s M)_o\right)^{1/2} \tag{C9}$$

since both mass and density were determined after fixed periods of burning, but diameter was not directly measured except for a limited series of samples.

---

[8]For cylinders in cross flow, A is the product of length and diameter (D). While D changed, the length was essentially constant unless the piece fractured.

Table C-1.--*Firebrand burning rate data. Data are for ovendry limbwood samples, each initially 5 inches long*

Species of tree	Nominal diam.	Initial values		Final values		Derived values†		Wind-speed	Test time
		Mass	Density	Mass	Density	D/D_o	$\rho D/(\rho D)_o$		
	inches	g	g/cc	g	g/cc			mi/h	s
PP*	1	53.36	0.610	4.16	0.240	0.445	0.175	15	360
PP	1	47.20	.520	6.47	.260	.523	.262	15	300
PP	1	44.59	.584	5.32	.220	.562	.212	15	240
PP	1	31.33	.472	9.42	.239	.771	.390	15	180
PP	1	41.33	.559	13.31	.467	.621	.519	15	120
ES	1	48.44	.706	6.99	.329	.557	.259	15	360
ES	1	50.70	.755	9.69	.340	.652	.293	15	300
ES	1	45.41	.577	18.46	.307	.874	.465	15	240
ES	1	73.05	.779	28.39	.461	.810	.480	15	180
ES	1	74.60	.777	42.01	.600	.854	.659	15	120
WL	1	29.59	.564	2.74	.132	.629	.147	15	240
WL	1	21.15	.474	3.01	.128	.726	.196	15	180
WL	1	23.00	.475	7.08	.230	.796	.387	15	120
WRC	1	51.14	.583	1.76	.099	.449	.077	15	300
WRC	1	42.41	.511	3.00	.118	.553	.128	15	240
WRC	1	46.25	.543	9.70	.277	.641	.327	15	180
WRC	1	40.38	.550	13.28	.300	.777	.423	15	120
PP	0.5	11.54	.536	0.76	.053	.815	.081	10	180
PP	.5	14.01	.660	2.85	.143	.968	.210	10	150
PP	.5	10.76	.547	2.13	.106	.010	.196	10	120
PP	.5	7.74	.347	2.33	.127	.907	.260	10	90
ES	.5	22.46	.786	2.16	.106	.844	.114	10	180
ES	.5	23.98	.746	3.86	.153	.886	.182	10	150
ES	.5	20.33	.696	2.60	.099	.949	.135	10	120
ES	.5	36.83	.750	16.85	.484	.842	.543	10	90
WL	.5	18.45	.468	1.71	.102	.652	.142	10	180
WL	.5	21.75	.699	5.16	.263	.794	.299	10	150
WL	.5	22.81	.623	5.26	.231	.789	.293	10	120
WL	.5	16.61	.485	9.01	.314	.915	.592	10	90
WRC	.5	20.25	.529	1.45	.077	.700	.102	10	180
WRC	.5	19.04	.529	2.51	.123	.752	.175	10	150
WRC	.5	18.93	.522	3.34	.214	.656	.269	10	120
WRC	.5	17.09	.585	3.09	.191	.745	.243	10	90

*PP = Ponderosa pine; ES = Engelmann spruce; WL = Western larch; WRC = Western red cedar.

†D/D_o = diameter ratio inferred from square root of mass ratio ÷ density ratio; $\rho D/(\rho D)_o$ = density ratio times diameter ratio.

Substantial scatter was evident in the data, and two sources of such scatter can be identified. In some trials not all of the sample burned. When only part of the length of the section burned, the final density and mass would be much greater than in those cases where the whole section burned. Also, in some trials (especially for longer burn times) the sample would burn through and pieces would be blown away. In these cases the final mass (but not final density) would be significantly lower than in cases that had whole samples at the end of the run. The records showing which tests suffered which defect (if any) were not available[9] at the time of this analysis, so all data were used, with the foreknowledge that the results would include significant variation. Figure C-1 illustrates the scatter mentioned.

Although not enough data are available yet to quantify the process, the burning of wood pieces under forced convection appears to proceed in three stages. In the first stage, the dimensions of the piece appear to change insignificantly, if at all, but the mass drops as the outer portions pyrolyze. In the final stage, the piece remaining is entirely reduced to char and mass loss proceeds from shrinkage of the size of the piece as it burns away by glowing combustion. Between these two stages a transition phase exists during which a char layer is being formed and being eroded simultaneously. Comprehensive models of this process have been attempted by several workers (see, e.g., Kanury 1974; Kung 1971) but they are so complicated that the level of refinement of the rest of this analysis precludes their use here. The simplistic model employed here should suffice for order-of-magnitude computation.

As shown on the graph of figure C-1, the regression coefficient value obtained was

$$b = K = 0.0064. \qquad \text{(C10)}$$

This number was used in deriving the maximum range formulas graphed in the text. Revision of this number by including more experimental data can easily be reflected in the results, as is shown in appendix F.

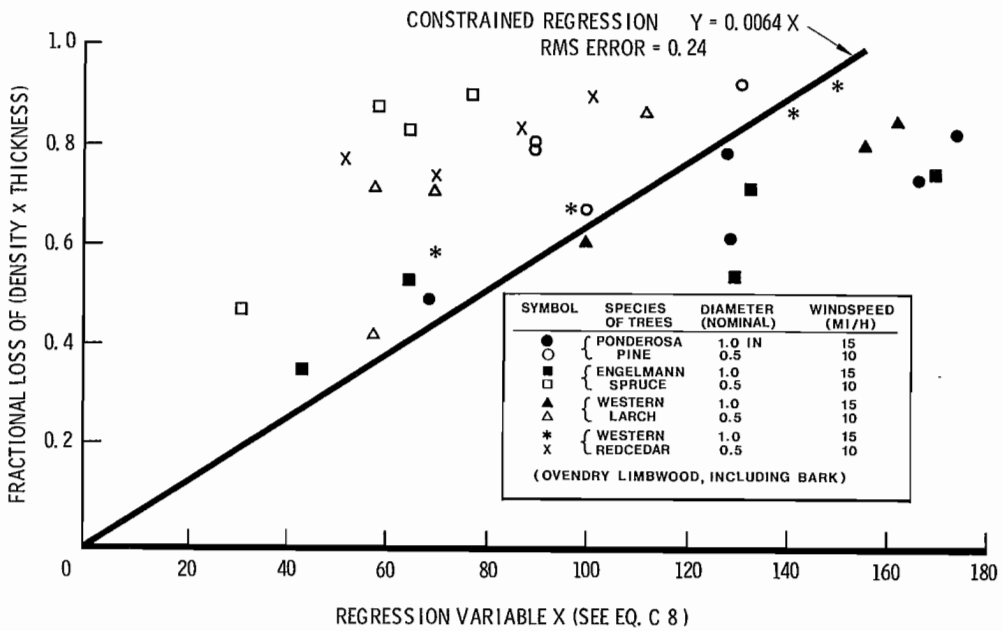

Figure C-1.--Data used to establish firebrand burning rate model.

[9]Records had been discarded for lack of storage space.

APPENDIX D: LOFTING OF FIREBRANDS BY FLAME AND BUOYANT PLUME

In this appendix a model is developed for the process by which potential firebrands are lofted into the buoyant plume above a steady flame. The flame is, of course, from a burning tree or group of trees, so is not truly steady, but transient. The flame/buoyant plume structure is treated as a steady flow field but is permitted to collapse, from the bottom upward, when the foliage of the burning tree(s) is consumed. The potential firebrand is represented in this model as an insert cylinder with specific gravity typical of weathered wood.

The analysis proceeds in three phases. First an approximate formula is developed for the velocity of a firebrand in the vertical flow field. This formula is then applied to derive the height of the particle as a function of time, assuming that the flow field is truly steady. The demise of the flow field is then approximated by using the steady state gas velocity versus height equations to predict the progress of the last bit of flame product upward through the flow structure. With the passage of this imaginary surface, the flow is presumed to be terminated as a coherent structure, leaving any particles "overtaken" to be transported by the wind field from the height at which they are when overtaken.

I. *Velocity of an Inert Particle in a Constant Vertical Flow Field*

The lifting of a potential firebrand by the flow field within and above a burning tree can be described approximately by considering an idealization of the process. The particle starts presumably from rest and is accelerated by aerodynamic drag upward against the pull of gravity. As will be shown below, particles that have terminal fall velocities not greatly different from the fluid velocity are accelerated rapidly (in a short distance as well as in a short time) to the speed at which the force of gravity is just balanced by the drag induced by its velocity relative to the gas. This fact leads to the useful approximation that the particle is borne by the (variable) flow field at such a speed as to produce the drag/gravity balance everywhere. So the first step in the model development is to describe the acceleration of an inert particle from rest by a constant flow field. The following variables are used in this description:

m = mass of inert particle
v = vertical velocity of particle
t = time
ρ = gas density
C_D = drag coefficient of particle
A = area presented to flow by particle
w = gas velocity (vertical)
g = acceleration of gravity.

The equation of motion can be written as

$$m \frac{dv}{dt} = \frac{1}{2} \rho C_D A (w - v)^2 - mg \qquad \text{(D1)}$$

and put in dimensionless form by defining the following variables:

$$v_o = \text{terminal fall velocity in still fluid} = (2mg/\rho C_D A)^{1/2} \tag{D2}$$

$$\theta = gt/v_o \tag{D3}$$

$$s^* = (w - v)/v_o = \text{normalized "slip velocity"} \tag{D4}$$

$$\frac{ds^*}{d\theta} = 1 - (s^*)^2. \tag{D5}$$

The slip velocity history given by integrating (D5) is

$$s^* = 1 + 2/\left(\left(\frac{w + v_o}{w - v_o}\right) \exp(2\theta) - 1\right) \tag{D6}$$

when the particle starts from rest at time t = 0. This equation shows that the ultimate slip velocity, v_o, is approached closely within a very brief period of time. For example, if v_o is 10 ft/sec, then in one second θ has a value of 3.2 and, even if w is very much greater than v_o, the slip velocity has fallen to within 0.3 percent of its "final" value. The distance covered in that time may be large, however, so (D6) must be integrated again to define the spatial history of the particle velocity. Denoting particle height by z, note that:

$$\frac{dz}{dt} = v = w - v_o s^*. \tag{D7}$$

In terms of dimensionless variables

$$z^* = gz/v_o^2 \tag{D8}$$

$$w^* = w/v_o \tag{D9}$$

and using (D6) for s^* we have

$$\frac{dz^*}{d\theta} = w^* - 1 - \frac{2(w^* - 1)\exp(-2\theta)}{(w^* + 1) - (w^* - 1)\exp(-2\theta)}. \tag{D10}$$

The last term in (D10) is a perfect differential, so

$$z^* = (w^* - 1)\theta - \ln\left((w^* + 1 - (w^* - 1)\exp(-2\theta))/2\right) \tag{D11}$$

if z is zero at time t = 0. Recasting (D6) in terms of the ratio of particle velocity to ultimate particle velocity,

$$v^* = v/(w - v_o) \tag{D12}$$

we can write the velocity and height equations as:

$$v^* = 1 - 2/((w^* + 1)\exp(2\theta) - (w^* - 1)) \tag{D13}$$

$$z^* = (w^* + 1)\theta + \ln(1 - v^*). \tag{D14}$$

These equations are graphed in figure D-1 as a crossplot of z* as a function of v*. For typical firebrand particles we are interested in "terminal velocity" values, v_o, of about 10 feet per second (Clements 1977). Figure D-2 shows actual vertical distances traveled by particles accelerated from rest in constant flow by the time they have achieved 90 percent of their ultimate velocities. This figure shows that particles of the type considered good candidates for firebrands achieve a "steady" slip velocity that balances the force of gravity in a very short distance in the flow conditions typical of the flames from burning trees (see appendixes A, B). Thus the approximation is made:

The particle everywhere travels at the velocity which balances drag and particle weight.

This approximation will overestimate the firebrand-lofting capability of any given flow structure, but not by a substantial amount. For particles traveling in spatially variable flows, this approximation greatly simplifies the analysis. The variable flow field of the flame/plume structure is addressed below.

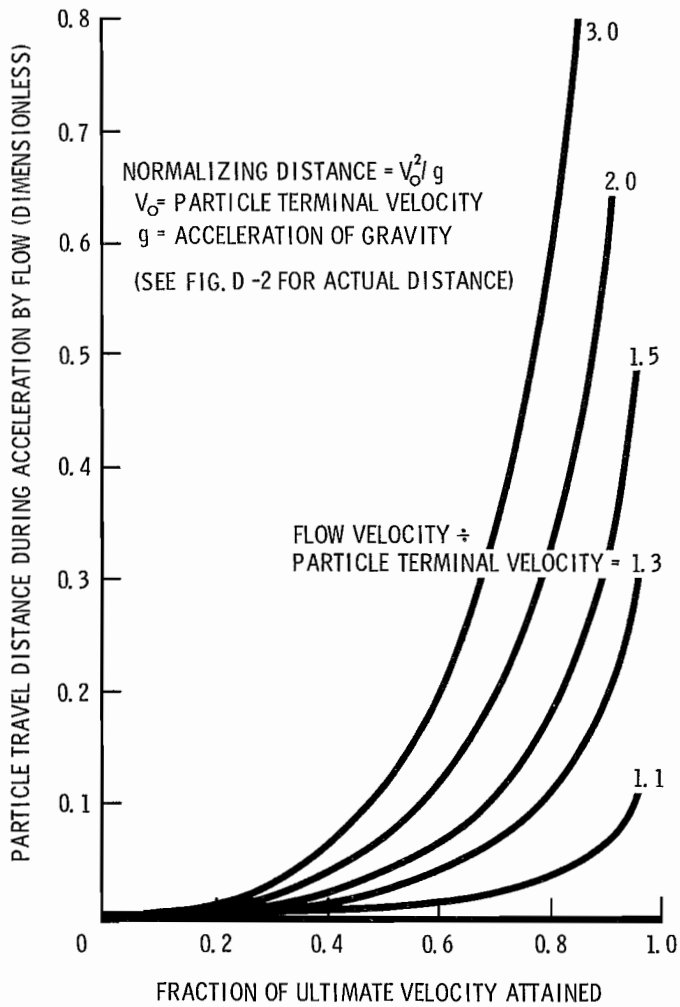

Figure D-1.--Distance traveled by particle accelerated upward from rest by constant-velocity flow.

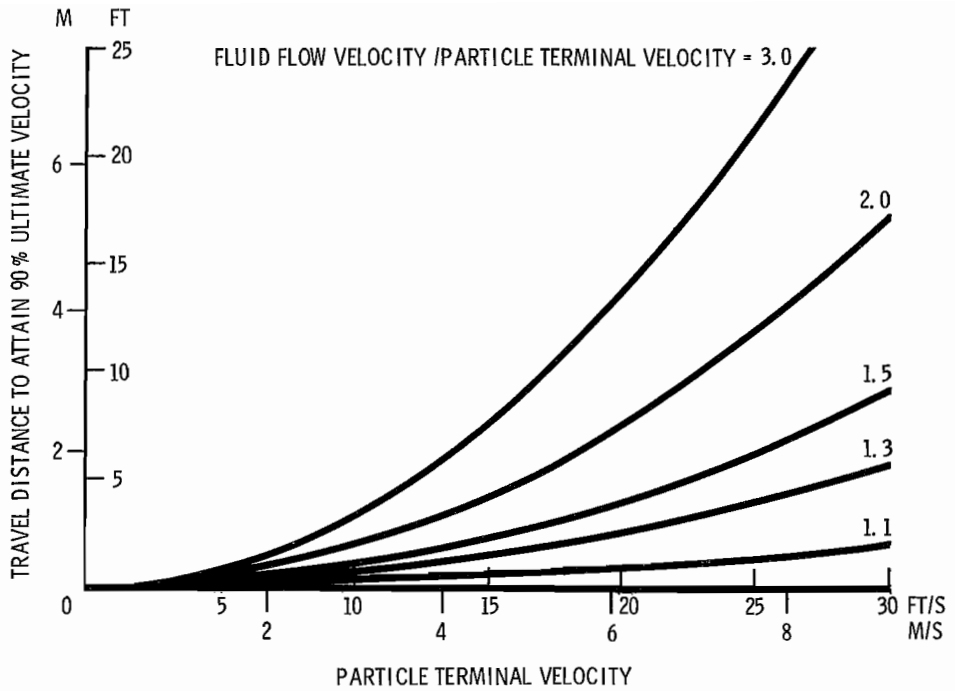

Figure D-2.--Distance required for particle to accelerate upward to 90 percent of ultimate velocity, starting from rest, in constant fluid flow.

II. *Particle Trajectories in Flame/Plume Flow Fields*

The motion of an inert particle entrained in the flow through the upper part of a steady flame is approximated here by the equation

$$\frac{dz}{dt} = w - v_o \tag{D15}$$

where the fluid velocity, w, is a function of height, z, but v_o is assumed to be constant. This implies that the density of the flame gas is constant. The variation of the density is minor (appendix A, eq. A49) and influences v_o only as the square root of density, so use of the flame-tip value is justified here. The variation of w with z is adequately described by the approximation

$$w = w_F(z/z_F)^{1/2} \tag{D16}$$

where the subscript F denotes flame tip value.

Equation (D15) is readily integrated to yield the time, t_F, required for the particle to travel from its initial height, z_o, to the flame tip:

$$\frac{w_F t_F}{2z_F} = 1 - (z_o/z_F)^{1/2} + \frac{v_o}{w_F} \ln\left\{\frac{1 - v_o/w_F}{(z_o/z_F)^{1/2} - v_o/w_F}\right\}. \tag{D17}$$

By using the expression for w_F developed in appendix A and by expressing v_o in terms of the diameter of a cylinder the pertinent times and physical sizes can be made more apparent:

$$v_o/w_F = B(D/z_F)^{1/2} \tag{D18}$$

where

$$B = \left(\frac{3\pi}{2C_D}\left(\frac{\rho_s}{\rho_a}\right)\Big/\left(1 - \rho_p/\rho_a\right)\right)^{1/2} \tag{D19}$$

and

$$\left.\begin{aligned} C_D &= \text{drag coefficient} = 1.2 \text{ for cylinder in cross flow}^{10} \\ \rho_s &= \text{density of cylinder} \\ \rho_a &= \text{density of ambient air} \\ \rho_p &= \text{density of flame gases at flame tip.} \end{aligned}\right\} \tag{D20}$$

The parameter group, $2z_F/w_F$, which divides the time in equation (D17) is the time required for fluid to travel from the base to the tip of the flame. This time is a characteristic scale time for the flow and is used frequently in this analysis to normalize travel time.

Using representative values for the densities in expression (D19)

$$\rho_s = 0.3 \text{ gm/cc} \quad (19 \text{ lb/ft}^3) \tag{D21}$$

$$\rho_a = 1.2 \times 10^{-3} \text{ gm/cc} \quad (0.075 \text{ lb/ft}^3) \tag{D22}$$

$$\rho_p/\rho_a = 3/8. \tag{D23}$$

The value of B is found to be about 40. This value was used to construct figure D-3. This figure shows the travel time from initial height (z_o) to flame tip as a function of D/z_F. The time becomes indefinitely large when the fluid velocity at the initial height approaches the terminal velocity of the cylinder in the flame gas. But for those cylinders that start at half the flame height or greater, the travel time is generally less than 1.5 unless the diameter is nearly equal to the value that will not permit the particle to be lifted by the flow.

In the "transition zone" between the tip of the flame and the buoyant plume, the particle's terminal velocity decreases because the fluid density increases, but the fluid flow velocity is essentially constant:

$$\frac{dz}{dt} = w_F - v_{ot} \tag{D24}$$

---

[10]Most objects, unless aerodynamically shaped for stable flight, will tend to assume the orientation that maximizes drag when in unconstrained flight. The drag coefficient for cylinders (or flat disks) to be used here is about 1.2.

where

$$v_{ot} = v_o(z_F/z)^{1/2} \tag{D25}$$

and v_o is the particle's terminal velocity in fluid with a density equal to that at the flame tip. The travel time, t_t, through the transition zone (from $z = z_F$ to $z = 1.4z_F$) is given by the integral of (D24). Expressed in dimensionless form as before this time is:

$$\frac{w_F t_t}{2z_F} = \frac{1}{2}\int_{z_F}^{1.4z_F} \left\{1 + \frac{v_o/w_F}{\left(\frac{z}{z_F}\right)^{1/2} - \frac{v_o}{w_F}}\right\}\frac{dz}{z_F} \tag{D26}$$

$$= 0.2 + \frac{v_o}{w_F} + \left(\frac{v_o}{w_F}\right)^2 \ln\left\{\frac{(1.4)^2 - v_o/w_F}{1 - v_o/w_F}\right\}. \tag{D27}$$

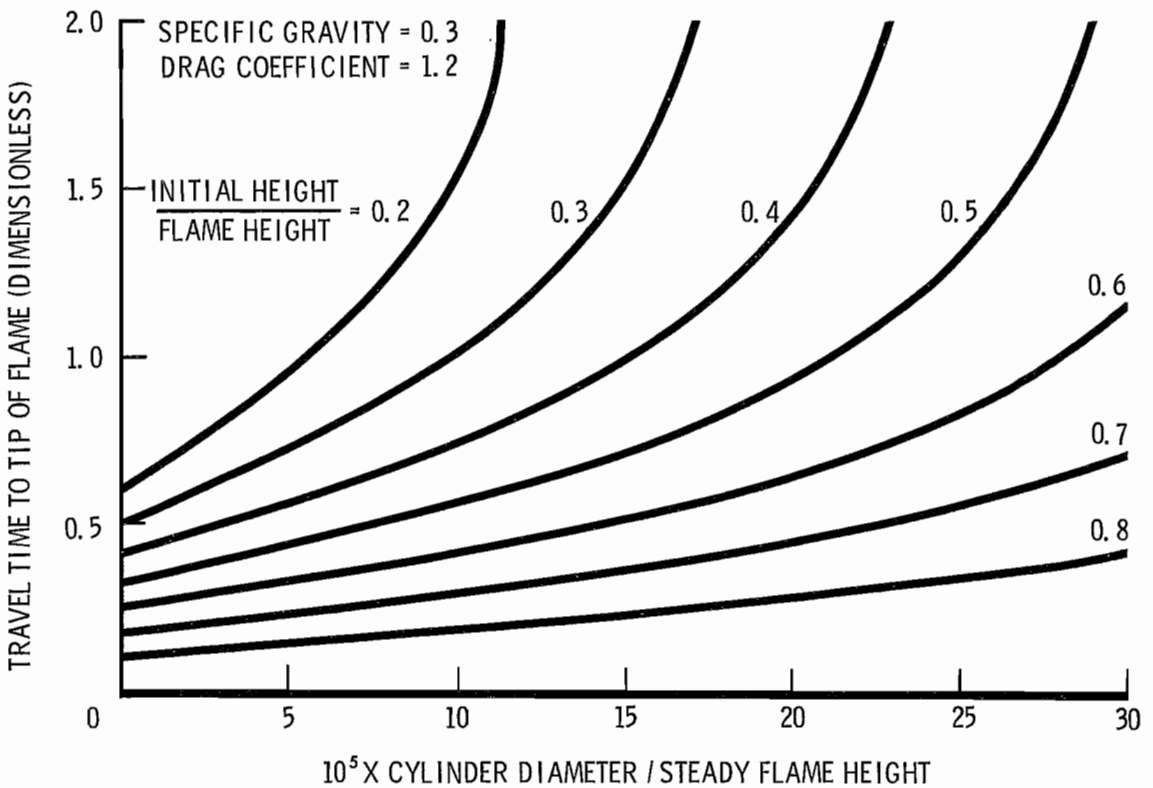

Figure D-3.--Approximate travel time for wood cylinder lifted by flame.

Since

$$v_o/w_F = B(D/z_F)^{1/2} \tag{D28}$$

and

$$(1.4)^2 \doteq 2, \tag{D29}$$

this can be written as

$$w_F t_t/2z_F \doteq 0.2 + B\left(\frac{D}{z_F}\right)^{1/2}\left\{1 + B\left(\frac{D}{z_F}\right)^{1/2} \ln\left(1 + 1/\left(1 - B\left(\frac{D}{z_F}\right)^{1/2}\right)\right)\right\}. \tag{D30}$$

This expression, like equation (D17), gives travel times near unity over the pertinent range of D/z_F. Figure D-4 is a graph of equation (D30).

To the travel times given in figures D-3 and D-4 must be added a travel time within the plume. This last time will be a function of the height to which the particle is lifted. Then by comparing the time it takes the particle to reach a particular height with the time the flow structure will persist to that height we can derive the maximum achievable height as a function of particle size.

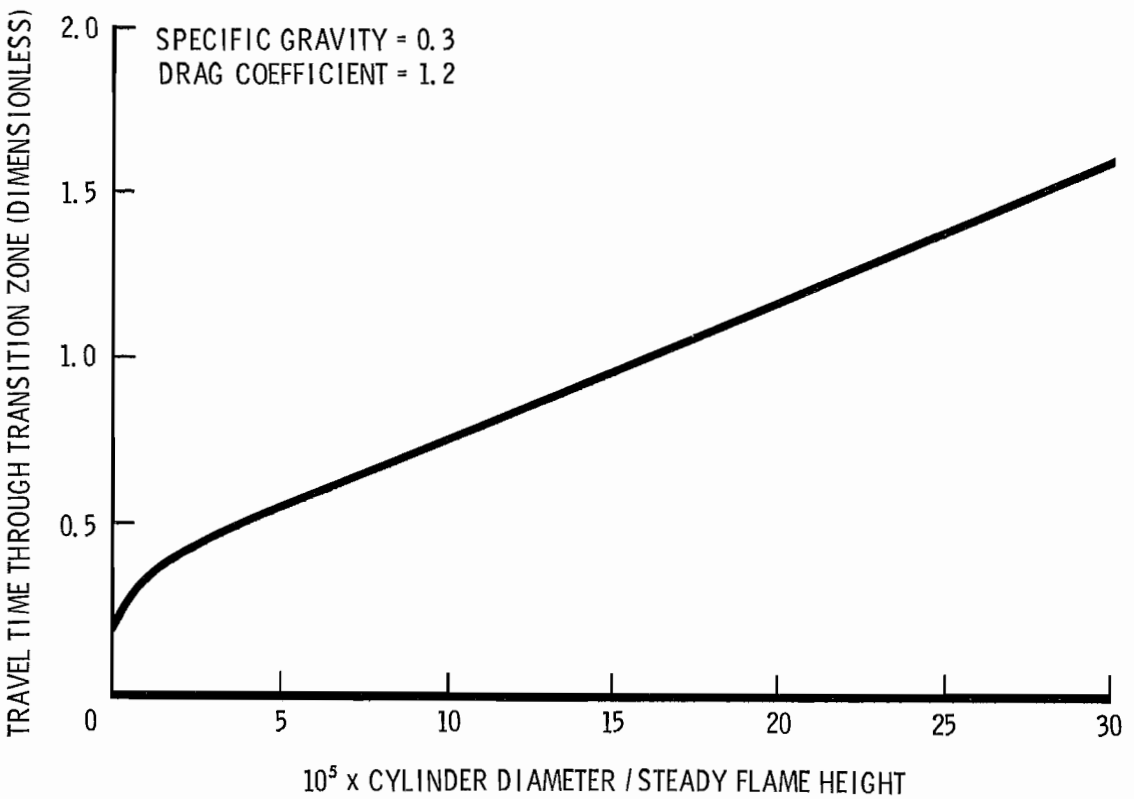

Figure D-4.--Approximate travel time for wood cylinder through transition zone between tip of flame and buoyant plume.

The flight of the particle in the buoyant plume is approximated here by

$$\frac{dz}{dt} = w - v_{op} \tag{D31}$$

where, from appendix B, the gas velocity is approximated by

$$w \doteq w_F(a/(b + z/z_F))^{1/2} \tag{D32}$$

with

$$a = 5.963 \tag{D33}$$

$$b = a - 1.4 = 4.563. \tag{D34}$$

The particle terminal velocity in the plume, v_{op}, is related to that in the flame, v_o, by

$$v_{op} \doteq 0.8v_o = 0.8Bw_F(D/z_F)^{1/2}. \tag{D35}$$

Again normalizing the particle height by the steady flame height and the time by the characteristic gas travel time through the flame, the time, t_p, required for a given particle to travel from the base of the plume ($1.4z_F$) to the height z can be written as

$$\frac{w_F t_p}{2z_F} = \frac{1}{2}\int_{a-b}^{z/z_F}\left(\left(\frac{a}{b + x}\right)^{1/2} - 0.8v_o/w_F\right)^{-1}dx. \tag{D36}$$

The result of the indicated integration in (D36) can be expressed conveniently in terms of the variable r, where

$$r = ((b + z/z_F)/a)^{1/2}. \tag{D37}$$

In terms of r, equation (D36) gives

$$\frac{w_F t_p}{2z_F} = \frac{a}{\left(0.8\frac{v_o}{w_F}\right)^3}\left\{\ln\left(\frac{1 - 0.8v_o w_F}{1 - 0.8rv_o/w_F}\right) - \left(0.8\,\frac{v_o}{w_F}\right)(r - 1) - \frac{1}{2}\left(0.8\,\frac{v_o}{w_F}\right)^2(r^2 - 1)\right\}. \tag{D38}$$

Again, using (D18) with a value of 40 for B, this formula can be used to calculate particle travel time in the plume. By combining the times given by equations (D38), (D30), and (D17) one obtains the total travel time from initial particle height, z_o, to the "final" height, z.

The contribution to this total time from the variation in initial particle height (figure D-3) complicates the calculation and presentation of the total time of travel. The refinement of a continuously variable initial height is clearly not warranted by the precision of the models presented here, either. So as a compromise between unwarranted generality and oversimplification, four representative values of z_o/z_F were chosen for display and further computation. Because the initial height of a firebrand particle would be no greater than the height of a tree contributing to the flame and because it has been assumed that the base of the flame is at one-half the tree height, the following representative values were chosen:

Tree Height/Flame Height (Range)	≤ 0.5	.5-1.0	1.0-1.5	≥ 1.5
Particle Initial Height/Flame Height (Range)	≤ 0.25	.25-.5	.5-.75	$\geq .75$
Nominal Value of z_o/z_F	0.2	0.4	0.6	0.8

These values probably typify the range of conditions to be encountered when single trees or groups of trees "torch out."

Using the nominal values for z_o/z_F in the tabulation above, figures D-5 through D-8 were constructed by adding the travel times from equations (D17), (D30), and (D38). Because the phase of travel from initial height to flame tip is a strong function of particle diameter for small values of z_o/z_F (i.e., for tall flames) the "resolution" in terms of D/z_F varies from one figure to another.

These figures provide the basis for a graphical solution of the firebrand lifting problem. The trajectories described by these four figures require that the gas flow exist over the height and time span indicated. So where the line describing the trajectory of the last bit of flame gas crosses one of the particle trajectories, it marks the maximum height achievable by a particle of the size associated with the intersected trajectory. The time required for the collapse of the flame/plume structure, in dimensionless units, is readily available from the equations already presented (D17, D30, and D38). One merely takes the limiting forms of these equations when the particle diameter approaches zero. Doing so gives the following results:

Time to travel from flame base ($z_o = 0$) to flame tip = t_1 (eq. D17)

$$t_1 = \lim_{\substack{v_o \to 0 \\ z_o \to 0}} \left(1 - \left(\frac{z_o}{z_F} \right)^{1/2} + \frac{v_o}{w_F} \ln \left(\frac{1 - v_o/w_F}{(z_o/z_F)^{1/2} - v_o/w_F} \right) \right) = 1. \qquad \text{(D39)}$$

Time to travel through "transition zone" = t_2 (eq. D30)

$$t_2 = \lim_{D \to 0} \left\{ 0.2 + B\left(\frac{D}{z_F}\right)^{1/2} \left(1 + B\left(\frac{D}{z_F}\right)^{1/2} \ln \left(1 + 1/\left(1 - B\left(\frac{D}{z_F}\right)^{1/2} \right) \right) \right) \right\} = 0.2. \qquad \text{(D40)}$$

Time to travel from plume base to height $z = t_3$. For this expression it is simpler to approach the limit in equation (D36) before integrating:

$$t_3 = \lim_{v_o \to 0} \frac{1}{2} \int_{a-b}^{z/z_F} \left(\left(\frac{a}{b + x} \right)^{1/2} - 0.8 \frac{v_o}{w_F} \right)^{-1} dx = \frac{1}{2} \int_{a-b}^{z/z_F} \left(\frac{b + x}{a} \right)^{1/2} dx \qquad \text{(D41)}$$

$$t_3 = \frac{a}{3} \left\{ \left(\frac{b + z/z_F}{a} \right)^{3/2} - 1 \right\}. \qquad \text{(D42)}$$

The total time for which the flow structure exists to height z, then is given by t_T, where

$$t_T = t_o + t_1 + t_2 + t_3 = t_o + 1.2 + \frac{a}{3} \left\{ \left(\frac{b + z/z_F}{a} \right)^{3/2} - 1 \right\}, \qquad \text{(D43)}$$

and t_o is the period of steady burning of the tree crown(s) normalized by the characteristic time $2z_F/w_F$. Equation (D43) is plotted[11] in figure D-9 on the same scale as figures D-5 through D-8, using various values for t_o. By overlaying figures D-5 through D-8 on this graph, one can derive the maximum particle height as a function of particle size and steady flame duration, t_o.

Alternatively, one may insert the values of t_T and z/z_F obtained from the particle trajectory figures into equation (D43) and derive the required flame duration, t_o. Using intermediate values not necessarily displayed in figures D-5 through D-8, figures D-10 through D-13 were derived in this way. These figures permit the final step in the long procedure outlined here--fixing the maximum height of viable firebrands.

Overlaid on these figures is the dashed line relating the initial diameter of a wood particle and the maximum height through which it may fall and yet be burning (glowing) on impact. This relationship, based on the wind model presented in appendix E and trajectory analysis described in appendix F, is:

$$\max(z) = 0.39 \times 10^5 D. \qquad \text{(D44)}$$

The initial particle height must be added to the height increment gained in the flame and plume, so the dashed line must intercept the solid lines at the points where

$$z/z_F = 0.39 \times 10^5 (D/z_F) - z_o/z_F. \qquad \text{(D45)}$$

The final result, a plot of the maximum viable particle height versus flame duration for the four initial heights, is given as figure 7 in the text.

---

[11] The plot is readily extended below $z/z_F = 1$; the functional form of t_1 for $z < z_F$ is a square root.

Figure D-5.--Total travel time for wood cylinder lifted by flame into buoyant plume. Initial particle height = 0.2 x steady flame height.

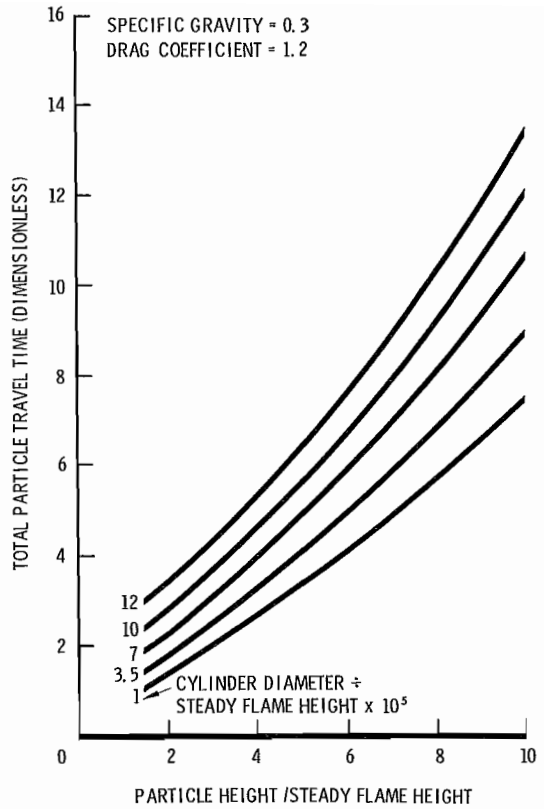

Figure D-6.--Total travel time for wood cylinder lifted by flame into buoyant plume. Initial particle height = 0.4 x steady flame height.

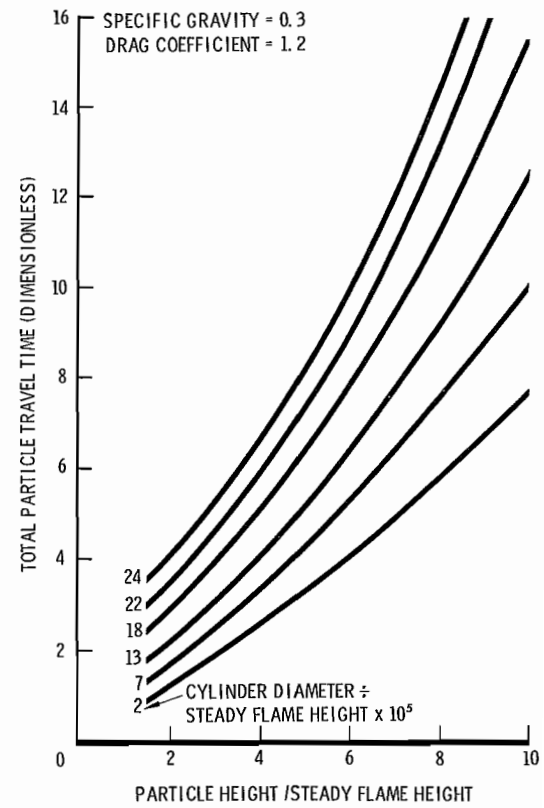

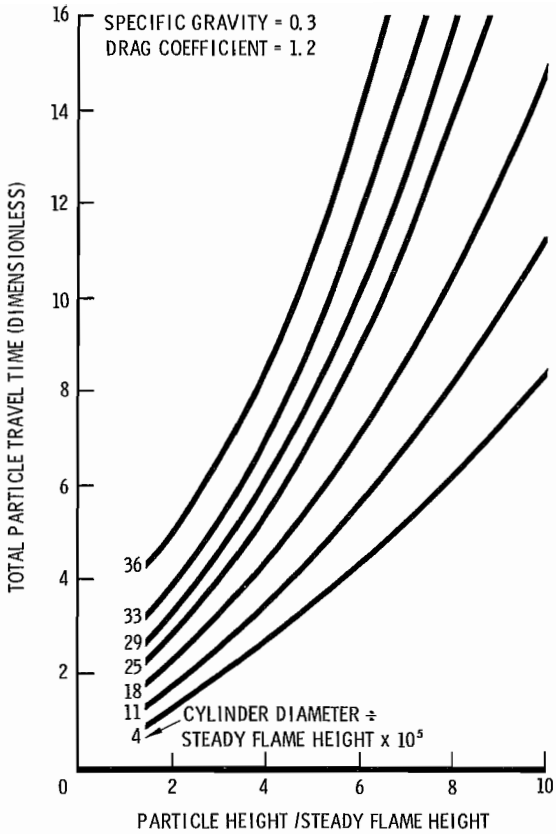

Figure D-7.--Total travel time for wood cylinder lifted by flame into buoyant plume. Initial particle height = 0.6 x steady flame height.

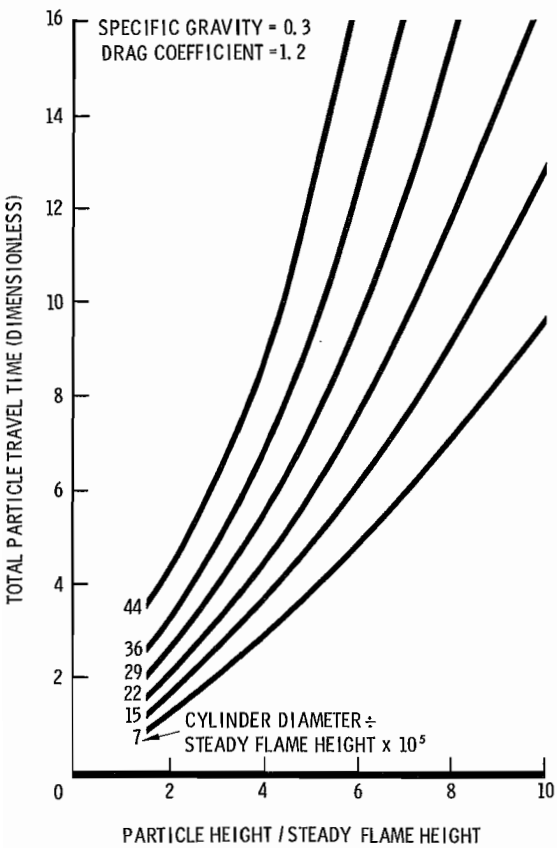

Figure D-8.--Total travel time for wood cylinder lifted by flame into buoyant plume. Initial particle height = 0.8 x steady flame height.

Figure D-9.--Total gas flow persistence time for buoyant plume above flame.

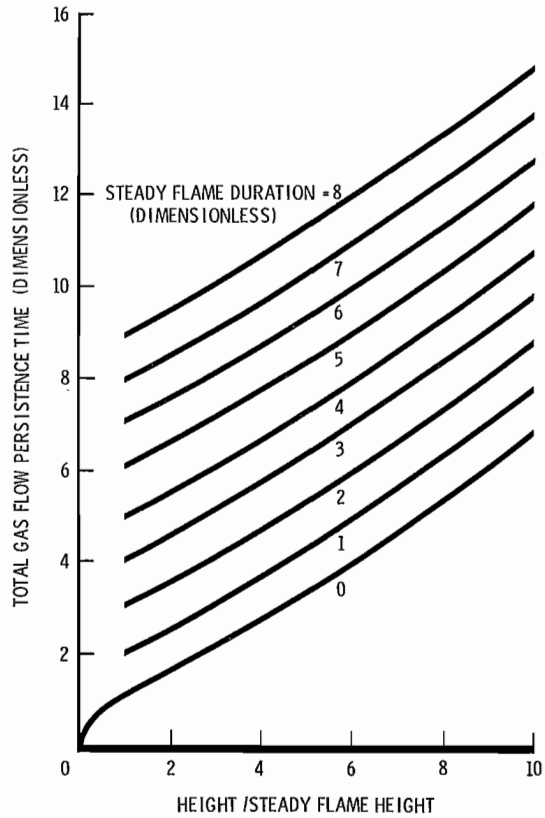

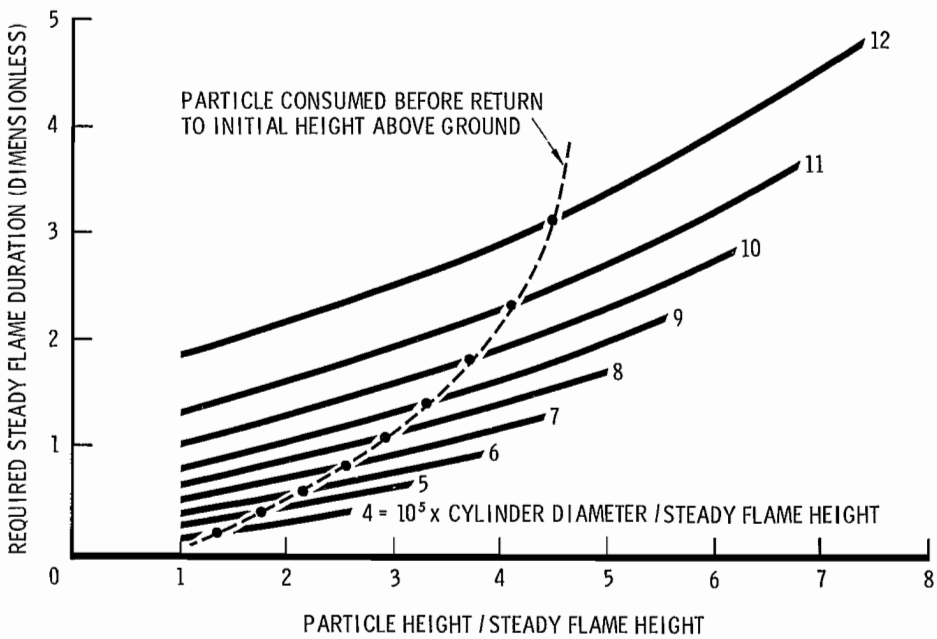

Figure D-10.--Flame duration required to lift wood cylinder to various heights, starting from 0.2 x steady flame height.

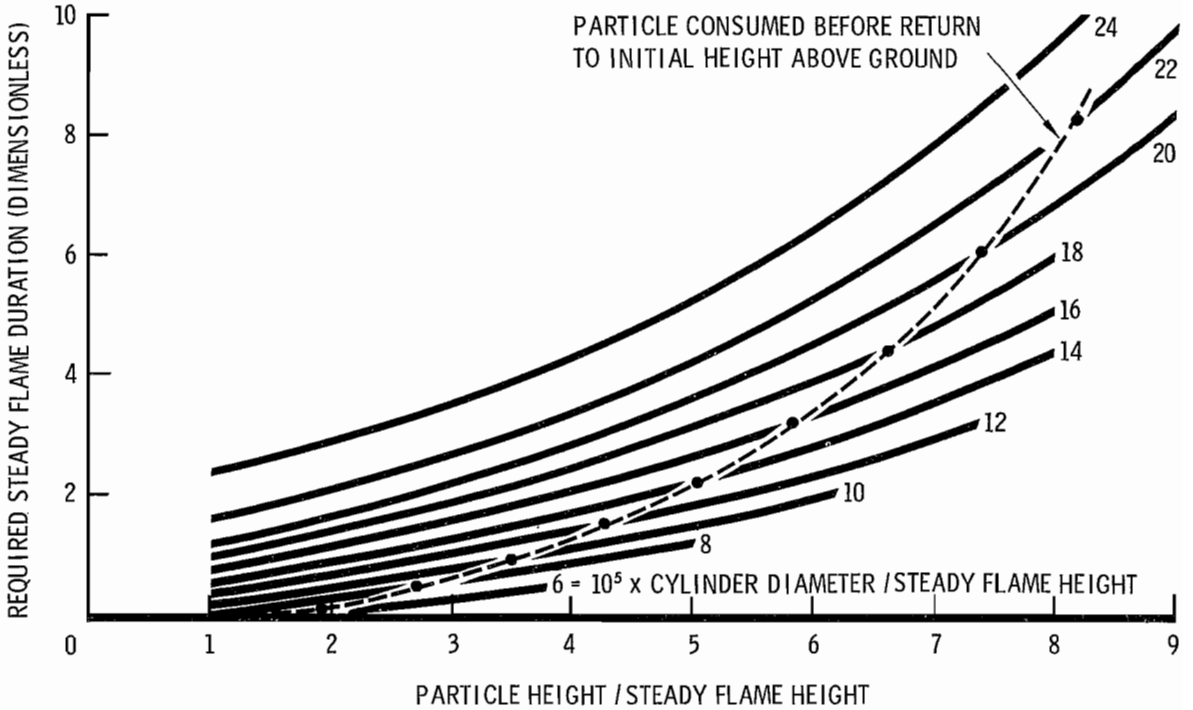

Figure D-11.--Flame duration required to lift wood cylinder to various heights, starting from 0.4 x steady flame height.

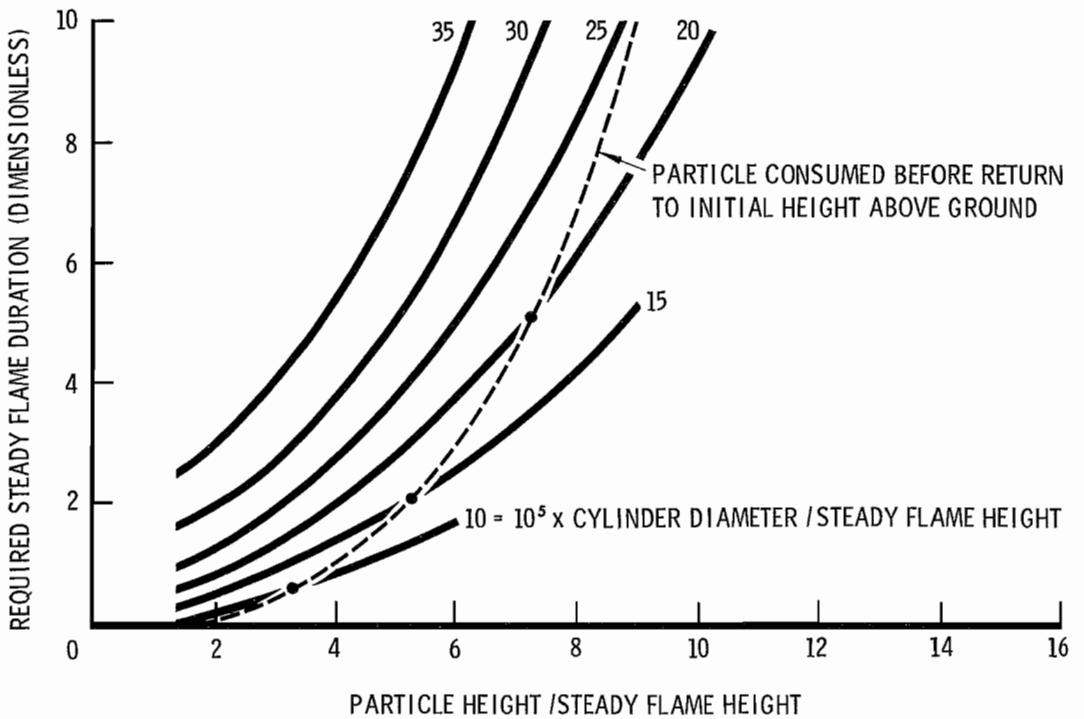

Figure D-12.--Flame duration required to lift wood cylinder to various heights, starting from 0.6 x steady flame height.

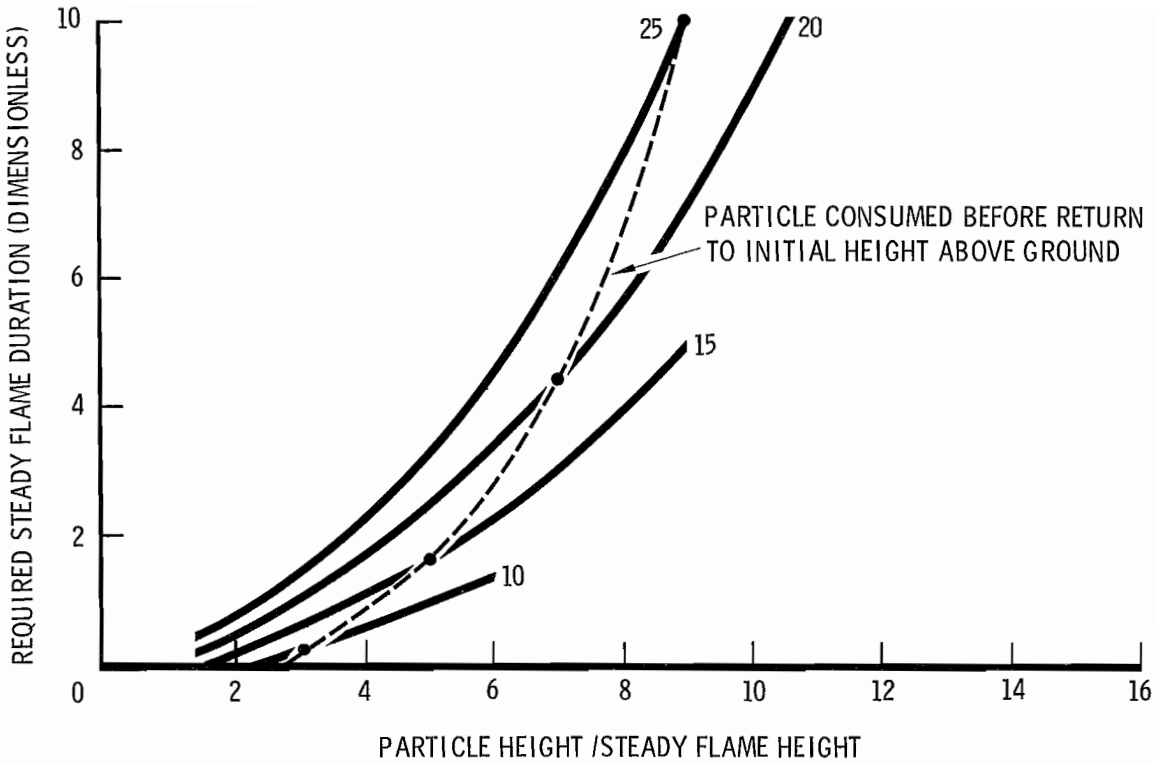

Figure D-13.--Flame duration required to lift wood cylinder to various heights, starting from 0.8 x steady flame height.

APPENDIX E: A CRUDE MODEL FOR SURFACE WIND OVER ROUGH TERRAIN

In order to calculate the distance that a firebrand might be carried by the wind, it is necessary to describe the wind field in detail. Such a description is clearly beyond the state of the art of meteorology when the problem is stated in general terms. That is, the details of the wind velocity pattern over rough terrain for arbitrary atmospheric conditions are not predictable at the present time. But since we are concerned only with making rather crude "limiting" calculations, it is sufficient for the purpose at hand to describe the general features of the flow field in some typical situations. The crude model should reflect the influence of the terrain and the roughness of the surface cover on the windspeed, but it is not necessary that the model be forecastable or even relatable to atmospheric transport processes. It need only be descriptive, and correct in the sense and approximate magnitude of factors that influence the wind pattern.

Two idealized situations are used here to typify the spotting problem:

1. The terrain can be considered to be flat in the direction of the prevailing wind.

2. The wind blows directly across a "smooth" ridge/valley profile that represents the major terrain relief in the area of concern.

These two situations obviously do not exhaust the possibilities, but until the entire spot fire model is validated to some degree in these easily described situations there seems little point to complicating the picture further.

The first case is intended to represent not only genuinely flat or gentle terrain, but airflow up or down drainages. The second case is intended to represent a typical fire control problem--spotting over a ridgetop or valley floor fuel break.

For the "flat terrain" case we shall use only a horizontal wind component. The windspeed near the surface, above the canopy of a forested area, is well described by a logarithmic profile (Sutton 1953; Marunich 1975):

$$U = (U_*/K)\ln(z/z_o) \tag{E1}$$

where

U = horizontal windspeed (short term average)
z = height above ground
z_o = "roughness length," a linear scale associated with the turbulent transport of shear stress
U_* = "friction velocity," a characteristic windspeed
K = von Karman's constant, usually reckoned at 0.4.

Data presented by Marunich (1975) and Tanner and Pelton (1960) indicate that the roughness length is related to tree height for wind over a uniform-height forest canopy. These data provide the following values:

$$z_o = 0.1313H \tag{E2}$$

$$U_* = 0.16U\big|_{z=1.6H} \tag{E3}$$

where H = tree height.

Other surface covers give rise to other (smaller) friction lengths (Sutton 1953).

Referring velocities to the value just at treetop height, U_H, gives

$$U = U_H \ln(z/0.1313H)/\ln(1/0.1313) = 0.493U_H \ln(z/0.1313H). \quad \text{(E4)}$$

This is the form used in the calculation of firebrand transport presented in the text.

For the second case, the matter is not so simple. In this case the velocity of the wind in the vertical direction (W) must be taken into account, as well as the variation of windspeed with height (z) and horizontal distance (X). It has often been noted that windspeed is greater at ridgetops than at midslope, and greater there than on the valley floor (Sutton 1953). The modeling of these variations has met with little success (Brown 1974) and is the subject of current research and development effort (Fosberg and others 1976; Ryan 1977).

Here we wish to capture only the gross features of such variations in a simple form. To do this we posit an oversimplified physical picture of the flow field over the rough terrain. The physical assumptions of this model are:

1. There exists an inviscid flow field trapped between an isobar at (constant) height z_G and a friction-dominated surface layer of height $z_{FR}(X)$.

2. The flow fields in both the inviscid upper layer and the friction layer are two-dimensional. That is, velocity exists in the X direction (U) and the z direction (W) only.

3. The friction layer boundary, $z_{FR}(X)$, is a streamline below which the horizontal velocity is logarithmic in z with a constant roughness length, z_o. No stability correction is applied.

4. The flow satisfies the incompressible continuity equation everywhere and air density variations are neglected.

5. Horizontal velocity is independent of height in the inviscid layer. In crude form, then, this model mimics some major features of Fosberg's (1976) model. In the model presented by Fosberg it is suggested that the "lid" height, z_G, should be taken to be 1.5 to 2.0 km above the mean height of the terrain. For the purpose of presenting numerical results in this paper we take z_G to be 6,000 ft (about 1.8 km) above the mean terrain height.

The flow field resulting from the above assumptions can be derived in a straightforward way. First, in the inviscid upper layer we have:

$$U(X) \cdot \left(z_G - z_{FR}(X)\right) = \text{constant} = V_G. \quad \text{(E5)}$$

From the continuity equation

$$\frac{\partial U}{\partial X} + \frac{\partial W}{\partial z} = 0 \quad \text{(E6)}$$

this implies a vertical velocity distribution

$$W(X,z) = -\left[V_G z/(z_G - z_{FR})\right]^2 \frac{dz_{FR}}{dX} + f(X). \tag{E7}$$

The arbitrary function f(X) is determined by matching the upper boundary condition that z_G is constant, a horizontal streamline:

$$W(X,z) = \left[\frac{V_G(z_G - z)}{(z_G - z_{FR})^2}\right]\frac{dz_{FR}}{dX} = U\left[\frac{z_G - z}{z_G - z_{FR}}\right]\frac{dz_{FR}}{dX}. \tag{E8}$$

In the friction layer between the terrain surface, $z_T(X)$, and the streamline $z_{FR}(X)$, we have

$$U = \frac{U_*(X)}{K} \ln\left(\frac{z - z_T(X)}{z_o}\right). \tag{E9}$$

The arbitrary friction velocity allows the matching of horizontal windspeed at the friction layer upper boundary, with the result:

$$U = \frac{V_G}{z_G - z_{FR}(X)} \ln\left(\frac{z - z_T(X)}{z_o}\right) \Big/ \ln\left(\frac{z_{FR}(X) - z_T(X)}{z_o}\right). \tag{E10}$$

The vertical velocity field in the friction layer is to be found by integrating the continuity equation. The result can be abbreviated as:

$$W = U\frac{dz_T}{dX} - z_o \frac{dF}{dX} \int_1^{(z-z_T)/z_o} \ln y \, dy, \text{ where} \tag{E11}$$

$$F(X) = \frac{V_G}{z_G - z_{FR}(X)} \ln\left(\frac{z_{FR} - z_T}{z_o}\right). \tag{E12}$$

Equation (E11) satisfies the boundary condition at the terrain surface ($z = z_T + z_o$); by imposing the boundary condition at the top of the friction layer

$$W(X,z_{FR}) = U(X,z_{FR})\frac{dz_{FR}}{dX} \tag{E13}$$

we obtain an equation describing the dependence of z_{FR} on z_T. This equation is

$$\frac{dz_{FR}}{dX} = \frac{dz_T}{dX} - z_o(z_G - z_{FR}) \int_1^{\frac{z_{FR}-z_T}{z_o}} \ln y \, dy \, \frac{d}{dX}\left((z_G - z_{FR})\ln\left(\frac{z_{FR} - z_T}{z_o}\right)\right)^{-1}. \tag{E14}$$

The dependence of z_{FR} on z_T can best be deduced by relating two intermediate variables:

$$f = (z_{FR} - z_T)/z_o \tag{E15}$$

$$g = (z_G - z_{FR})/z_o \tag{E16}$$

$$\frac{df}{dX} = -g\int_1^f \ln y \, dy \, \frac{d}{dX}\left(\frac{1}{g \ln f}\right). \tag{E17}$$

Carrying out the indicated differentiation and rearranging terms this becomes an easily integrated form:

$$\ln f \, \frac{df}{dX} \Big/ \int_1^f \ln y \, dy - \frac{1}{f}\frac{df}{dX} \Big/ \ln f = \frac{dg}{dX}/g \tag{E18}$$

$$\ln\left\{\int_1^f \ln y \, dy\right\} - \ln\{\ln f\} = \ln g + \text{constant} \tag{E19}$$

or

$$\int_1^f \ln y \, dy / g \ln f = \text{constant} = C. \tag{E20}$$

This last form is most revealing if cast in terms of the ratio of friction layer thickness to total (friction plus inviscid) layer thickness

$$\Phi = \frac{z_{FR} - z_T}{z_G - z_T} = f/(f + g) \tag{E21}$$

$$\Phi = \left(C - 1/(g \ln f)\right)/\left(C + 1 - (1 + \tfrac{1}{g})/\ln f\right). \tag{E22}$$

Because both f and g are large numbers relative to unity, equation (E22) provides the extremely useful result, that Φ may be considered to be constant. From equation (E20) it is clear that C (and hence Φ) is a small number. In fact, Sutton (1953) cites data taken over flat terrain that indicate $\Phi = 0.12$. Brown (1974) "splices" friction layer profiles to Ekman layer profiles and asserts that this layer depth ratio should be of the order of 0.1. In numerical results presented herein we have used $\Phi = 0.12$.

A further simplification obtains from this result and equation (E11). Note from (E11) that the relationship between W and U in the friction layer varies between the limits

$$W = U\frac{dz_T}{dX} \quad \text{at } z = z_T + z_o \tag{E23}$$

and

$$W = U\frac{dz_{FR}}{dX} = (1 - \Phi)U\frac{dz_T}{dX} \quad \text{at } z = z_{FR}. \tag{E24}$$

Because the "error" is so slight and the simplification is so great in the particle trajectory equations, the further approximation is made that the streamlines follow the terrain contour in the friction layer:

$$W \doteq U \frac{dz_T}{dX}. \tag{E25}$$

From equations (E5), (E8), and (E10) it is also clear that the friction layer equations for U and W can be extended into the inviscid zone for a distance equal to a large fraction of the friction layer height before significant error accumulates. This approximation is also invoked in deriving the firebrand trajectories in appendix F.

The variation of horizontal wind velocity with distance (U(X)) is plotted in figure E-1 for terrain described by a sinusoid:

$$z_T(X) = a \sin (\pi X/X_o). \tag{E26}$$

The total terrain relief, 2a, is a parameter for these curves. The curves plotted are given by equation (E10) with

$$(z_{FR} - z_T)/(z_G - z_T) = 0.12 \tag{E27}$$

and z_G equal to 6,000 ft above the average value of z_T. This plot shows that for a ridge-to-valley elevation change of 2,000 ft, the velocity at a constant height above the terrain differs by about 40 percent between ridge and valley locations. It is this variation of horizontal windspeed with horizontal distance that causes the differences in potential spotting distances shown in the graphs in the text.

To facilitate transformation of windspeed measurements or forecasts (to establish the midslope reference value of treetop height wind), the variation of horizontal windspeed with terrain elevation is graphed in the text.

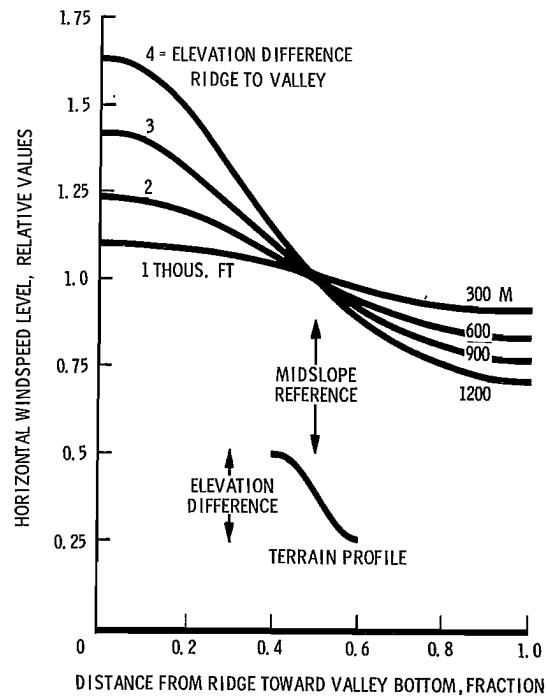

Figure E-1.--Variation of horizontal windspeed at constant height above terrain for flow across ridge and valley. Model results for sinusoid terrain profile and uniform forest cover, 100 ft (30 m) trees.

APPENDIX F: FIREBRAND TRAJECTORIES

In this appendix we combine the model for the burning of wood cylinders (appendix C) and the model for the windspeed over rough terrain (appendix E) to calculate the maximum possible travel distance of such particles. This is done in two steps. First we compute the maximum spot fire distance over flat terrain, then we calculate a correction factor for rough terrain.

Using the approximation that the particle everywhere has a relative velocity in the vertical direction equal to its instantaneous terminal fall velocity (appendix D) we can write the equations of motion for the burning firebrand as follows:

$$\frac{dX}{dt} = U(X,z) \tag{F1}$$

$$\frac{dz}{dt} = W(X,z) - v_o(t). \tag{F2}$$

Here we use the symbols

X = horizontal distance
z = vertical distance
t = time (since start of firebrand fall)
U = horizontal windspeed
W = vertical windspeed
v_o = particle terminal fall velocity, a function of t.

The fact that the relative velocity of the particle with respect to the wind is everywhere equal to v_o allows us to obtain the time dependence of v_o directly. From appendix C we have the model

$$\frac{d}{dt}(\rho_s D) = -K\rho_a v_o \tag{F3}$$

where

K = 0.0064
ρ_s = density of wood cylinder
D = mean diameter of wood cylinder
ρ_a = density of air
v_o = relative velocity of cylinder and air (here equal to terminal velocity).

But since the terminal velocity is given by

$$v_o = (\pi g \rho_s D/2C_D\rho_a)^{1/2} \tag{F4}$$

where

g = acceleration of gravity
C_D = drag coefficient (1.2)

equation (F3) can be written in terms of v_o:

$$\rho_s D = 2C_D \rho_a v_o^2 / \pi g \tag{F5}$$

$$(4C_D \rho_a v_o / \pi g) \frac{dv_o}{dt} = -K \rho_a v_o \tag{F6}$$

$$\frac{dv_o}{dt} = -K\pi g / 4C_D . \tag{F7}$$

This leads immediately to a most useful result:

$$v_o(t) = v_o(0)\left(1 - K\pi g t / 4C_D v_o(0)\right) . \tag{F8}$$

In other words, the particle slows down its relative fall velocity linearly in time. During the time it burns out, it moves a distance Δz relative to the air in which it is borne along, where

$$\Delta z = \frac{1}{2} v_o(0) \left[\frac{4C_D v_o(0)}{K\pi g} \right] = (\rho_s D)_o / K\rho_a \tag{F9}$$

and

$(\rho_s D)_o$ = the initial value of $(\rho_s D)$.

Because, according to the wind model derived in appendix E, streamlines near the surface are parallel to the terrain surface, this "fall distance" is a constant of the trajectory and is equal to the initial height of the particle if the particle burns out on returning to the surface. This fact was used in appendix D to identify those particles that have the greatest potential spot distance.

Using the shorthand notation

$$\tau = 4C_D v_o(0) / K\pi g \tag{F10}$$

equation (F2) can be written

$$\frac{dz}{dt} = W(X,z) - v_o(0)(1 - t/\tau) . \tag{F11}$$

Flat Terrain Spot Distance

Equations (F1) and (F11), with U given by a logarithmic function of z and W equal to zero, describe the flight of a firebrand over flat terrain:

$$\frac{dX}{dt} = \left(U_*/K\right) \ln(z/z_o) \tag{F12}$$

$$\frac{dz}{dt} = -v_o(0)(1 - t/\tau) . \tag{F13}$$

The logarithmic profile does not accurately describe windspeed variation below treetop height. Although such windspeed variations have been measured many times (Baynton 1965; Bergen 1971; Fons 1940; Gisborne 1941; Leonard and Federer 1973; Martin 1971; Marunich 1975; Oliver 1971; Raynor 1971), no universal rule is applicable because of the many factors that can influence the wind field structure within and below the crown layer. One approximation for the purpose at hand would be to use a constant windspeed below treetop height. This would give a maximum spot fire distance, but perhaps one unrealistically large. Another approach would be to consider the crown layer as a mechanical obstacle to the flight of a firebrand and set the windspeed to zero below treetop height. Such an approximation would tend to give a lower bound to the spot fire distance. A compromise that interpolates between these extremes is to extend the logarithmic profile below treetop height all the way to zero velocity. This is the alternative used here. The effect of this assumption is assessed later in this appendix.

Denoting treetop height by H and the horizontal windspeed at that height by U_H, equation (F12) can be written as

$$\frac{dX}{dt} = U_H \ln(z/z_o)/\ln(H/z_o). \tag{F14}$$

The friction length, z_o, is set to 0.1313H for the calculation of numerical results. The treetop height, and hence z_o, is considered to be constant over the range of particle travel.

Equation (F13) can be integrated to give the particle height as a function of time:

$$z(t) = z(0) - v_o(0)\tau\left(t/\tau - \frac{1}{2}(t/\tau)^2\right). \tag{F15}$$

Because we seek the maximum spot fire distance, the particle should just be consumed at the time of contact with the ground, or

$$z(\tau) = 0 \tag{F16}$$

and so

$$z(t) = z(0)(1 - t/\tau)^2. \tag{F17}$$

Using this result in equation (F13) and dividing equation (F14) by the resulting expression gives the equation for the particle's distance of travel (X) as a function of its height (z):

$$\frac{dX}{dz} = -\left(\frac{U_H}{v_o(0)}\right)\left(\frac{z(0)}{z}\right)^{1/2} \ln(z/z_o)/\ln(H/z_o). \tag{F18}$$

This equation is readily integrated to give the maximum horizontal distance X*. When normalized by the tree height the result is:

$$X^*/H = \frac{4U_H}{v_o(0)} \frac{(z_o z(0))^{1/2}}{H \ln(H/z_o)} \left\{\left(\frac{z(0)}{z_o}\right)^{1/2}\left(\frac{1}{2}\ln\left(\frac{z(0)}{z_o}\right) - 1\right) + 1\right\}. \tag{F19}$$

Since

$$\ln(H/z_o) = -\ln(0.1313) = 2.03, \tag{F20}$$

this expression is very well approximated by the form

$$X^*/H \doteq \frac{2U_H}{v_o(0)} \left(\frac{z(0)}{H}\right)^{1/2} \left\{(0.1313)^{1/2} + \frac{1}{2}\left(\frac{z(0)}{H}\right)^{1/2} \ln\left(\frac{z(0)}{H}\right)\right\}. \tag{F21}$$

If the integral on z had been terminated at H rather than at z_o (zero windspeed below treetop height) the term $\sqrt{0.1313}$ would be missing from this expression. And if the windspeed were set to a constant for z less than H, the term $\sqrt{0.1313}$ would be replaced by unity. Figure F-1 shows how the results would change, using the constant windspeed (maximum range) assumption as a reference condition for comparison.

Using equation (F9) for $v_o(0)$ in terms of z(0) (= Δz) and using numerical values for the constants gives the equation plotted as a nomograph in the text:

$$X^* = 21.9U_H\left(\frac{H}{g}\right)^{1/2} \left\{0.362 + \left(\frac{z(0)}{H}\right)^{1/2} \frac{1}{2} \ln\left(\frac{z(0)}{H}\right)\right\}. \tag{F22}$$

This result is more cogent than it may appear at first, since a multiplying factor can extend the validity of the expression to uneven terrain.

Uneven Terrain Spot Distance

The flight of a firebrand over uneven terrain is described by equations (F1) and (F16) when the wind field is related to the terrain surface. Using the wind model described in appendix E and especially the approximation that the streamlines parallel the terrain, we can write the equation for particle height as a function of time:

$$\frac{dz}{dt} = U \frac{dz_T}{dX} - v_o(t) \tag{F23}$$

where $z_T(X)$ = terrain height at location X.

Because the particle travels horizontally at speed U, the height of the particle above ground obeys the simple equation

$$\frac{d}{dt}(z - z_T) = -v_o(t) = -v_o(0)(1 - t/\tau). \tag{F24}$$

The simplification made possible by this result is enormous. Because the horizontal windspeed is related to the height above the local terrain:[12]

$$\frac{dX}{dt} = U(X,z) = \frac{v_G/\ln\left(\phi \dfrac{z_G - z_T}{z_o}\right)}{(1 - \phi)(z_G - z_T)} \ln\left(\frac{z - z_T}{z_o}\right) \tag{F25}$$

---

[12]See appendix E for definition of symbols ϕ, z_G, and v_G.

and since

$$z - z_T = \left(z(0) - z_T(X = 0)\right)(1 - t/\tau)^2 = z^0(1 - t/\tau)^2 \tag{F26}$$

equation (F23) is essentially the same as equation (F14). If the treetop height windspeed, U_H, is considered to be a function of horizontal position, the equations are identical. The integral form for the maximum spot distance is obtained as before. Using equation (F26) in (F24) and dividing (F25) by the result yields:

$$\frac{dX}{d(z - z_T)} = - \frac{\left(v_G/v_o(0)\right)\ln(H/z_o)\cdot\left(z^0/(z - z_T)\right)^{1/2}\ln\left((z - z_T)/z_o\right)}{(1 - \phi)(z_G - z_T)\ln\left(\phi(z_G - z_T)/z_o\right)\ln(H/z_0)}. \tag{F27}$$

The integral of the function of $(z - z_T)$ on the right gives a function of initial particle height above the ground (z^0) and tree height that is identical to the previous case. Hence we have:

$$\frac{1 - \phi}{v_G \ln \frac{H}{z_o}} \int_0^{X^*} (z_G - z_T)\ln\left(\frac{\phi(z_G - z_T)}{z_o}\right)dx = \frac{2H}{v_o(0)}\left(\frac{z^0}{H}\right)^{1/2}\left\{0.362 + \frac{1}{2}\left(\frac{z^0}{H}\right)^{1/2}\ln\left(\frac{z^0}{H}\right)\right\}. \tag{F28}$$

This formula should, of course, reduce to the flat terrain form simply by setting z_T equal to a constant. By choosing the constant value to be the spatial average terrain height, denoted by $\bar{z}_T$, we derive the ratio formula for the maximum spotting distance in the form:

$$\int_0^{X^*} \frac{z_G - z_T}{z_G - \bar{z}_T} \frac{\ln\left(\phi \frac{z_G - z_T}{z_o}\right)}{\ln\left(\phi \frac{z_G - \bar{z}_T}{z_o}\right)} dX = X^*(\text{flat terrain}). \tag{F29}$$

The right hand side of equation (F29) is the maximum spot fire distance over flat terrain *using the windspeed (as a function of height) that obtains at the average terrain height.*

The integral in this equation can be simplified by considering only cases for which

$$|z_T - \bar{z}_T|/(z_G - \bar{z}_T) << 1; \tag{F30}$$

for these cases, since

$$(z_G - z_T)/(z_G - \bar{z}_T) = 1 + (\bar{z}_T - z_T)/(z_G - \bar{z}_T), \tag{F31}$$

$$\ln\left(\phi \frac{z_G - z_T}{z_o}\right) \doteq \ln\left(\phi \frac{z_G - \bar{z}_T}{z_o}\right) + \frac{\bar{z}_T - z_T}{z_G - \bar{z}_T} \tag{F32}$$

and so

$$X^* + \int_0^{X^*} \left(1 + 1/\ln\left(\phi \frac{z_G - \bar{z}_T}{z_o}\right)\right) \frac{\bar{z}_T - z_T}{z_G - \bar{z}_T} \, dX \doteq X^*(\text{flat terrain}). \tag{F33}$$

The variation of terrain height relative to the average height can be represented with good generality by a sinusoid,

$$z_T - \bar{z}_T = a \sin (m(X + X_1)) \tag{F34}$$

where

$2a$ = total elevation difference, ridge to valley

$m = \pi \div$ horizontal distance from ridge to valley

X_1 = horizontal location of firebrand source ($X_1 = 0$ is midslope on windward side of ridge).

This form leads to a transcendental equation for the maximum horizontal distance:

$$X^* + \frac{(1 + \alpha)a}{m(z_G - \bar{z}_T)} \left\{\cos (m(X^* + X_1)) - \cos (mX_1)\right\} = X^*(\text{flat terrain}) \tag{F35}$$

where

$$\alpha = 1/\ln(\phi(z_G - \bar{z}_T)/z_o). \tag{F36}$$

Equation (F35) was solved for the ratio of maximum distances and plotted in the text. The four cases presented in the text correspond to different values of mX_1. The values used are as follows:

mX_1	*Location of firebrand source*
π	midslope on lee side of ridge
$-\pi/2$	valley bottom
0	midslope on windward side of ridge
π	ridgetop

For the numerical results plotted in the text, the value of α was set to 0.2 and $z_G - \bar{z}_T$ to 6,000 ft. These values, along with $\phi = 0.12$ (see appendix E), imply a roughness scale of $z_o = 4.9$ ft. The weak dependence of the resulting ratio of maximum ranges on the parameter a implies that the numerical value of α is not critical in this range of values. The location of the firebrand source is very important, however.

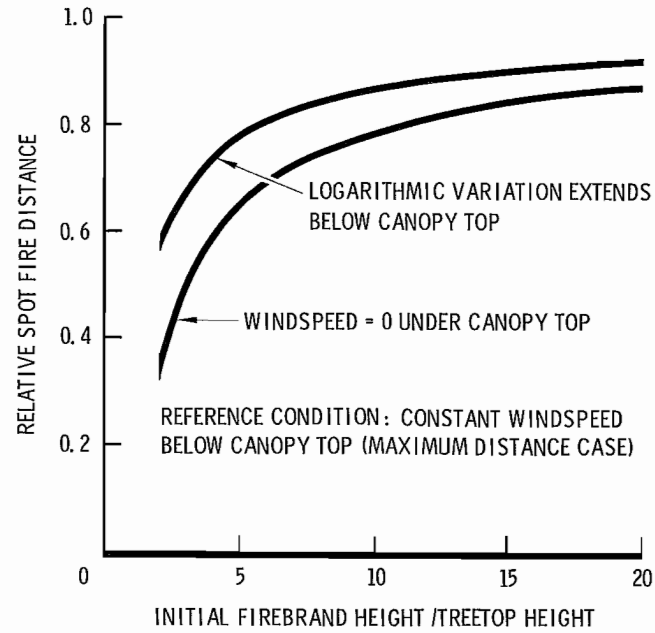

Figure F-1.--Effect of different windspeed profiles on predicted maximum spot fire distance.

Burning Rate Model Influence

Note that if the firebrand burning rate were different from the model used here (i.e., if a different value of the burning rate regression parameter b of appendix C were used) only the value of τ would be changed. The scaling relationships would be preserved between flat terrain and uneven terrain results. The impact of a change in the burning rate would be to change the numerical coefficient K in equation (F9) and hence the value of the coefficient in equation (F22). The number 21.9 in the latter equation is inversely proportional to the square root of the burning rate coefficient K, so results for spot fire distance should be altered accordingly to reflect a different K value.

☆U.S. GOVERNMENT PRINTING OFFICE: 1979-0-677-019/12

ALBINI, F. A.
1979 Spot fire distance from burning trees--a predictive model
USDA For. Serv. Gen. Tech. Rep. INT-56, 73 p. Intermt. For. and Range Exp. Stn., Ogden, Utah

Presents a predictive model for calculating the maximum spot fire distance expected when firebrands are thrown into the air by the burning of tree crowns. Variables included are: quantity and surface/volume ratio of foliage in the burning tree(s), height of the tree(s), and the wind field that transports the firebrands, and the firebrand burning rate. No validation data are available at present.

KEYWORDS: Predictive model, spot fire distance, firebrands.

ALBINI, F. A.
1979 Spot fire distance from burning trees--a predictive model
USDA For. Serv. Gen. Tech. Rep. INT-56, 73 p. Intermt. For. and Range Exp. Stn., Ogden, Utah

Presents a predictive model for calculating the maximum spot fire distance expected when firebrands are thrown into the air by the burning of tree crowns. Variables included are: quantity and surface/volume ratio of foliage in the burning tree(s), height of the tree(s), and the wind field that transports the firebrands, and the firebrand burning rate. No validation data are available at present.

KEYWORDS: Predictive model, spot fire distance, firebrands.

Headquarters for the Intermountain Forest and Range Experiment Station are in Ogden, Utah. Field programs and research work units are maintained in:

Billings, Montana
Boise, Idaho
Bozeman, Montana (in cooperation with Montana State University)
Logan, Utah (in cooperation with Utah State University)
Missoula, Montana (in cooperation with University of Montana)
Moscow, Idaho (in cooperation with the University of Idaho)
Provo, Utah (in cooperation with Brigham Young University)
Reno, Nevada (in cooperation with the University of Nevada)